Rare Met. (2023) 42(3):769–796
https://doi.org/10.1007/s12598-022-02142-7

RARE METALS

REVIEW

Recent progress of transition metal-based biomass-derived carbon composites for supercapacitor

Ya-Nan Zhang*, Chen-Yang Su, Jun-Lei Chen, Wen-Huan Huang*, Rui Lou

Received: 25 January 2022 / Revised: 12 May 2022 / Accepted: 20 May 2022 / Published online: 24 November 2022

Abstract Supercapacitors (SCs) have been considered as the most promising energy storage device due to high power density, long cycle life, and fast energy storage and efficient delivery. The excellent electrode materials of SCs generally have based on large porous structure, excellent conductivity, and heteroatom doping for charge transfer. Among various electrode materials, biomass-derived carbon materials have received widespread attention owing to excellent performances, environmental friendliness, low-cost and renewability. Additionally, composites materials based on biomass-derived carbon and transition metal-based material can obtain more advantages of structural and performance than single component, which opens up a new way for the fabrication of high-performance SC electrode materials. Therefore, this review aims to the recent progress on the design and fabrication of biomass-derived carbons/transition metal-based composites in supercapacitor application. Finally, the development trends and challenges of biomass-derived electrode materials have been discussed and prospected.

Keywords Biomass-derived carbon; Transition metal composites; Supercapacitor (SC); Electrochemical

Y.-N. Zhang*, C.-Y. Su, J.-L. Chen, W.-H. Huang*, R. Lou
Shaanxi Key Laboratory of Chemical Additives for Industry, College of Chemistry and Chemical Engineering, Shaanxi University of Science and Technology, Xi'an 710021, China
e-mail: zhangyanan@sust.edu.cn

W.-H. Huang
e-mail: huangwenhuan@sust.edu.cn

1 Introduction

With the rapid development of the energy industry, more and more attentions focused on the advanced electrochemical energy conversion or storage devices with a high performance, such as fuel cells, batteries, supercapacitors (SCs) (Scheme 1) [1–3]. SCs are the most promising energy storage systems due to higher power density (~ 10 $kW{\cdot}kg^{-1}$), long cycle life, and fast energy storage and efficient delivery [4–6]. Based on energy storage mechanisms, SCs are divided into two categories: electric double layer capacitors (EDLCs) and pseudocapacitors. EDLCs mainly rely on the electrostatic adsorption from electrolyte ions on the electrode/electrolyte interface to store energy, obtaining rapid charge and discharge rate. Compared with EDLCs, pseudocapacitors mainly utilize faradaic charge transfer reaction caused by electroactive materials on the surface of the electrode to storage higher capacitance and energy density than EDLCs [7, 8]. In general, most of EDLC electrode materials are from versatile carbonaceous materials, such as carbon blacks (CB), activated carbon (AC), carbon nanotubes (CNT), graphene (GN), and carbon nanofibers (CNFs) [9–12]. Carbon-based materials, especially porous carbon, display higher surface areas, adjusting pore distributions and morphology, good conductivity and stability to improve the capacitance of EDLCs. Besides, the heteroatom doping on the carbon is beneficial to change the electronic and crystal structure and improve chemical stability and electrical conductivity, producing pseudocapacitive response [13–16]. Therefore, with the development of electrochemical energy storage technology, plenty of well-defined nanostructured carbon materials have been carried out in SCs by researchers. However, most carbon-based nanomaterials currently rely heavily on expensive raw precursors and complicated energy-

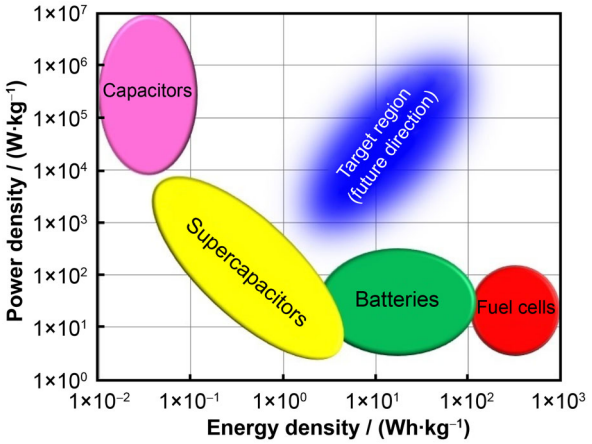

Scheme 1 Scheme of electrochemical energy conversion and storage devices. Reproduced with permission from Ref. [2]. Copyright 2021, Wiley online

consuming synthetic conditions. By the way, their synthetic process inevitably brings the environment pollution [17–20].

Recently, biomass-derived carbon materials have received widespread attention as SCs electrode materials owing to excellent performances, environmental friendliness, low-cost and renewability. Additionally, well-developed porous structure, active surface, good chemical stability and heteroatom-doped chemical composition of biomass-derived carbon are beneficial to get high specific capacity as electrode materials. Generally speaking, a large number of biomass resources have been simply burned to generate energy in the past, and this low-efficiency energy utilization have brought serious environment problems, that is in contradiction with social sustainable development demands, therefore, it is necessary to find an efficient way to utilize biomass resource. So far, the effective approach is to convert the carbon stored in biomass into carbon-based functional materials, which opens up a new avenue for converting biomass into value-added products. To date, various studies have been explored to obtain carbon functional material from biomass as SCs electrode with different nanotechnologies, such as pyrolysis, high temperature carbonization, self-activation, and self-assembly [21–27]. Through green and facile nanotechnologies, the exquisite and complicated hierarchical nanostructure and morphologies have been fabricated to provide more channels for conducting ions and electrons. Thus, biomass-derived carbon can be commonly used as an anode for asymmetric supercapacitors due to its wide potential windows, physical chemistry stability and ease of fabrication, improving the capacitance of EDLC.

Compared with EDLCs, the pseudocapacitance electrode shows higher energy density due to surface-faradaic/pseudo-faradaic reactions. The conventional pseudocapacitive electrode materials generally include conductive polymers, transition metal oxides (TMO), transition metal sulfides (TMS), transition metal hydroxides (TMH), metal-organic frameworks (MOFs), etc. [28–38]. However, the capacities of pure metal-based electrode perhaps have been restricted by the poor active sites, the aggregation of metal nanoparticles, volume expansion during charge-discharge cycles and structural damage in the faradic processes [39–41]. To solve the above problems, the hybrid electrodes that take full advantages of EDLC and pseudocapacitance have been paid more and more attention. Interestingly, the conductive carbons as substrate provide rich nucleation sites for the growth of pseudo-capacitive materials and expand the electrical active region and conductivity, that is convenient for charge transfer and full utilization of the active material [42]. More importantly, the carbon matrix alleviates the structural damage of pseudo-capacitive material in cycling, and the interaction between the carbon surface and pseudocapacitance function groups is beneficial to reduce interfacial resistance and keep structural integrity. Therefore, given the advantages of nanocomposites fabricated by carbonaceous materials and metal compounds in SCs, this review aims to the recent progress on the design and synthesis of biomass-derived carbons/transition metal-based composites in supercapacitor application in the past years. And then the development trends and challenges of new electrode materials have been discussed and prospected.

2 Synthesis of biomass-derived carbon for SCs electrode materials

Biomass-derived carbon can be considered as ideal choice in the application of SC electrode material because of its excellent conductivity, enriched porosity and physicochemical stability. However, untreated biomass precursors contain too much impurity to be used as a material for supercapacitors. The biomass-derived carbon after treatment presents large specific surface area (SSA), adjustable porous structure, heteroatom doping, fascinating nanostructures and excellent conductivity. Thus, in order to obtain suitable pore distribution, modulate the surface chemistry and design nanostructures of biomass-derived carbon, the biomass carbonization technologies have been utilized for the fabrication of high-performance SCs. In carbonization process, the biomass precursors undergo a series of transformations under inert atmosphere below 800 °C to increase the carbon content. The thermal conversion involving pyrolysis and hydrothermal carbonization (HTC) is considered to be the most efficient method to remove H, O, N, and S in biomass and produce high-value-added activated carbon nanomaterials [43, 44]. Furthermore, to

increase surface area of carbon materials and adjust meso/micropore proportion after carbonization, activation methods (physical activation and chemical activation) have been proposed [45]. Sometimes, the combination of these methods can also improve the properties of biomass-derived carbon in electrochemical energy storage devices [46]. The related carbonization technologies have been proposed in many reports, so a brief overview is stated in this review.

2.1 Pyrolysis

Up to now, pyrolysis is the most direct way to receive biomass-derived carbon due to its flexibility and adjustable synthetic conditions, which divided into direct pyrolysis and activation [46, 47]. In direct pyrolysis, the raw biomass material is decomposed to gases, liquid biooil and carbon-rich biochar in an inert environment at the temperature range of 300–1000 °C, and the slow pyrolysis is beneficial to yield higher biochar production due to slower heating rate and longer reaction time. Meanwhile, the release of gas and decomposition of organic compounds can lead to the production of micropores structures, but the micropores formed by high-temperature pyrolysis exhibit lower surface area and poor pore structure, that is not conducive to rapid ion transport in electrochemical application. Therefore, the direct pyrolysis method is difficult to gain superior biochar materials with tunable porosity and excellent electrochemical performance [48]. As mentioned above, the activation in pyrolysis can be used to adjust the internal pore structure of biochar materials by etching, including physical activation and chemical activation.

The physical activation generally occurs in the presence of steam, air, O_2, CO_2, and mixed atmosphere, in which the fascinating porous channels are created inside the carbonaceous material with the carbonization and reaction of oxidizing atmosphere. In steam activation, when the activation temperature is higher than 900 °C, the reaction is not homogeneous because of excessive steam diffusion, however, the slow entry of water vapor into the pores of carbide particles under lower temperature is beneficial to facilitate a uniform and complete carbonization reaction [49]. The activation rate of CO_2-activation is slower than that of water vapor, so a higher temperature (800–1100 °C) is required for CO_2-activation process [50]. Beyond that, the conventional gas-activation need longer reaction time and more stringent experiment conditions, that cause uniform heating on the surface and inside of sample and affect the efficiency of activation and pore quality of carbon materials [51]. Different to gas-activation, microwave pyrolysis is a new carbonization activation technology to prepare biomass-derived carbon materials, and lots of heat is generated to promote high-speed molecular motion through microwave transmission at a high frequency. Simultaneously, the temperature increases rapidly and uniformly during the microwave reaction to effectively result in the formation of porosity in carbon materials [52–54]. As mentioned before, the porous carbonaceous materials derived from biomass prepared by physical activation have higher yield and simple synthesis technique, but such materials have a lower specific surface area and pore volume because of low carbon corrosion in the gas phase. Therefore, physical activation method is difficult to tune properties of the electrochemistry and surface chemistry in carbon material compared to chemical activation [55]. The chemical activation method refers to mix chemical activator with raw biomass under the protection of inert gas and heated at high temperature. Common chemical activators used are KOH, $ZnCl_2$, H_3PO_4, and so on, and other used activators such as H_2SO_4, K_2CO_3, $KHCO_3$, NaOH, and their mixtures have been reported rarely. For alkali activation, when KOH is used as activator, potassium-containing species gradually corrode the carbon matrix, generating plenty of micro/mesopores structures. In the carbonization process, the gasification of carbon can also generate numerous pores. Furthermore, metallic K is embedded into the skeleton of carbon matrix to expand the carbon lattices, resulting in higher porous structures and optimized electrochemical performance [56]. Furthermore, $ZnCl_2$ can act as chemical activator to produce porous carbon with different morphologies and high SSA, because the existing of $ZnCl_2$ is beneficial to accelerate dehydration at low temperature and depolymerization reactions at high temperature to increase carbon yields. However, the release of HCl may result in corrosion during the activation process and the relative activation is still being explored. Compared to $ZnCl_2$, H_3PO_4 activation has been widely applied in the industrial production due to low cost and high carbon yields. During activation process, H_3PO_4 can accelerate the hydrolysis and dehydration of raw materials, and the pores are constructed by removing phosphoric acid [57]. Up to now, the reaction mechanism of physical and chemical activation for producing porous carbon from biomass materials is worth exploring. Meanwhile, it faces great challenges to adjust porous structure of biomass-derived carbon by direct carbonization and/or activation process for improving the electrochemical performance.

2.2 Hydrothermal carbonization

HTC is a method to convert biomass materials into hydrochar structures. Various microporous structures have been fabricated by HTC method at the temperature range of 175–300 °C with an aqueous medium and high pressure.

Water is used as catalyst and solvent to promote hydrolysis and breakage of biomass chemical structure at high temperature [58]. Along with the temperature up to 200 °C, most of organic compounds in biomass are converted into high carbon materials, and their porosity of biomass-derived carbon increases accordingly. Compared to pyrolysis method, the target product is synthesized by aqueous medium and lower temperature to reduce pollution and energy consumption. Moreover, hydroxyl and carboxylic functional groups left on the surface of biomass-derived material are favorable for heteroatomic doping to promote the electrochemical properties. However, direct HTC easily leads to inhomogeneous porosity, thus the post-temperature activation method is used to adjust porosity, modify the surface chemical properties and enhance the graphitization of biomass-derived carbon [59].

3 Biomass-derived carbon composites for SC electrode materials

Compared to biomass-derived biochar material, composites materials based on porous carbon and metallic-based material can obtain more advantages of structural and performance than single component. The porous carbon derived from biomass material can provide plenty of room to deposit pseudocapacitive materials and effectively resist volume changes in the galvanostatic charge-discharge (GCD) process of electrochemical cycling performance to increase the conductivity. In the meanwhile, uniformly distributed metallic-based material within the carbonaceous skeleton improves the ability of redox reactivity. Compared to pure carbon-based materials, transition metal-based materials show higher capacitance through reversible faradaic reactions between electrode materials and electrolyte ions and better electrochemical stability for storing more energy. In addition, the multiple oxidation states of transition metal-based materials can effectively improve electron transmission for longer discharge time to enhance the energy density. The transition metal-based materials mainly include manganese, iron, cobalt, nickel, mixed metals, etc. They play a crucial role in improving the capacitance of electrode through fast faradaic pseudocapacitance effect. Recently, more researches focus on TMO, TMS, layered double hydroxides (LDH), metal-organic frameworks (MOFs), and they combine with capacitive electrode materials to construct hybrid supercapacitors for generating higher working potential and increasing charge storage. However, for transition metal-based materials, the lower specific surface area, weak intrinsic conductivity, and structural damage in cycling greatly limit electron transport and reduce cycle life. To overcome this problem, combining transition metal-based materials with biomass-derived carbon is an effective way to take advantages of these materials in electrochemical performance. Among them, carbon materials can provide enough space for depositing metal particles to enlarge active area. Meanwhile, the high conductivity of carbon can induce high rate performance and energy density [60–62]. Herein, in this review, we mainly discuss composite electrode materials based on biomass-derived carbon and transition metallic-based materials for SCs by different synthesis method (Scheme 2) [63–70].

4 Biomass-derived carbon/TMO composites

In this study, in supercapacitors, TMO have been demonstrated as typical pseudocapacitive materials due to high energy storage efficiency and fast ion adsorption at the electrode/electrolyte interface. Besides, multiple oxidation states of TMO determined the outstanding ability of redox reactivity. However, low porosity and structural damages greatly limited the ion transfer and reduced cycle life. Although the carbonaceous materials as EDLCs can improve the gravimetric energy storage ability, they performance inferior volumetric ability because of low packaging density. As a consequence, combining TMO and carbonaceous material from biomass to fabricate nanocomposites not only effectively enhances the capacitance of the carbon material, but also improves the conductivity of TMO. Beyond that, biomass derived porous carbon can also provide copious spaces for encapsulating

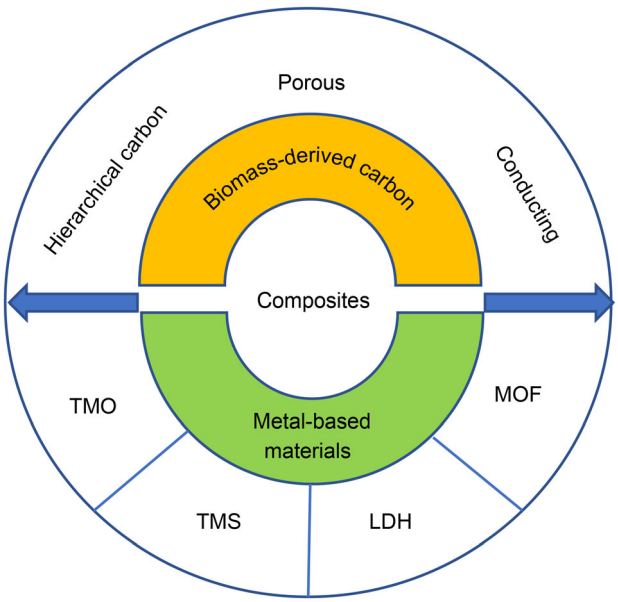

Scheme 2 Illustration of biomass carbon-based composites containing metal-based materials (TMO, TMS, LDH, MOF) for supercapacitor applications

TMO nanoparticles to increase the electrochemical active area and promote charge transfer. However, the loading of TMO on the carbon surface could lead to inhomogeneous distribution and low content of TMO, that is the biggest obstacle to the development of electrochemical properties of biomass-derived carbon/TMO composites. Therefore, the controllable design of nanostructured biomass-derived carbon/TMO composites is also a huge challenge [71–73]. To overcome the challenge, various methods have been tried such as morphological control, composite engineering, ingredient adjustment and interface control. For morphological control, integrated 3D core-shell heterostructure and hollow nanostructure of composites could provide more active sites and inhibit particle aggregation to improve electrochemical performance. Simultaneously, the electrochemical performance could be raised by improving interface between collector and electrode, mainly including element doping, surface modification, construction vacancies by carbon substrate. In addition, more efforts also need to be devoted to computationally-assisted design and synthesis of biomass-derived carbon/TMO electrode materials for better prediction of structure-activity relationship and reduction of synthetic attempts. In all, we still have a long way to go before biomass-derived carbon/TMO electrode materials can be actually used. The electrochemical parameters of main biomass-derived carbon/TMO used as the supercapacitor electrode materials are summarized in Table 1.

4.1 Biomass-derived carbon/manganese oxide composites

Manganese oxides (MnO_x) have been recognized as ideal candidates as pseudocapacitor materials in electrochemical application because of multiple oxidation state, high theoretical specific capacitance, eco-friendliness, low-cost, and abundant existing in nature. Among them, MnO_2 is an excellent candidate as electrode material due to its relatively high operating voltage and high theoretical capacitance ($\sim$1370 $F{\cdot}g^{-1}$). However, MnO_2-based material cannot perform satisfactory high specific capacity because of low electron-transporting capacity in application [74]. In general, the most feasible approach to solve this problem is the introduce of carbon material as conductive substrate to immobilize MnO_2 to increase its electrochemical conductivity and reduce the agglomeration. Up to now, many MnO_2/biomass-carbon nanocomposites in supercapacitor have been reported [75–77]. For example, biomass-derived porous carbon (BPC) from soybean stalk pieces with a large specific surface area of 1709.5 $m^2{\cdot}g^{-1}$ could densely and uniformly anchor birnessite-type MnO_2 nanoparticles (BPC/MnO_2), in which MnO_2 exhibited nanosheets and nanowires morphologies to facilitate penetration of electrolyte ion and increase exposure of electroactive sites via chemical activation and hydrothermal reaction. An all-solid-state asymmetric supercapacitor (ASC) device was fabricated to deliver high specific energy of 34.2 $Wh{\cdot}kg^{-1}$ and high specific power with 9.58 $kW{\cdot}kg^{-1}$ [78]. By the way, the electrochemical properties of the composites can be influenced by adjusting the crystalline phase and morphology of TMO. Yang et al. reported an enteromorpha prolifera-derived carbon substrate (ACEP) for direct growth of δ-MnO_2 and α-MnO_2 (Fig. 1) [79]. With the extension of reaction time, the metastable 2D nanosheets of δ-MnO_2 were transformed into stable 1D nanowires of α-MnO_2 (Fig. 1a, b). The ACEP@δ-MnO_2 as electrodes can be applied in asymmetric SC and exhibited a high energy density with 31.0 $Wh{\cdot}kg^{-1}$ at a power density of 500.0 $W{\cdot}kg^{-1}$ (Fig. 1c–g). The good electrochemical performance of ACEP@δ-MnO_2 is due to wider ionic diffusion channels of δ-MnO_2 nanosheets and the growth of δ-MnO_2 on carbon substrate to improve the conductivity and stability.

Although a large number of biomass-derived carbon/MnO_2-based electrode materials can improve the capacitance of the device as SCs, the instability and poor conductivity is still unsatisfied. To improve the electrochemical performance, introducing conductive polymers have become an effective method. Zhu et al. reported a flake-like MnO_2 nanostructure anchored on the ramie-derived carbon fibers (RCFs) by a facile electrodepositing process [80], then poly(3,4-ethylenedioxythiophene) (PEDOT) as a performance-booster was coated on the surface of MnO_2 via in situ polymerization to obtain RCFs/MnO_2/PEDOT hybrid electrode (Fig. 2a). In this process, the carbon fibers from ramie as a flexible skeleton provide an effective electronic transmission path, simultaneously, through the synergistic effect between MnO_2 nanoflakes and PEDOT wrapping layer, it can effectively enhance the conductivity and increase capacitance (Fig. 2b–e). As for RCFs/MnO_2/PEDOT hybrid electrode, it showed a high capacitance of 922 $F{\cdot}g^{-1}$ at 1 $A{\cdot}g^{-1}$ with 91% capacitance retention over 5000 cycles. Furthermore, the device can be bent easily, while electrochemical properties are not affected after 200 times bending (Fig. 2f–i).

In manganese oxides composites, electrode made of MnO-carbon composites (MnO/C) can also exhibit excellent electrochemical performance for supercapacitor with a high theoretical capacity to enhance the electrochemical activity of MnO and prevent the aggregation and erosion of MnO. However, most of biomass-derived carbons need carbonization and activation to present chunk, after that, MnO particles may be unevenly loaded on the surface of the carbon material. Therefore, it is necessary to explore a facile and effective method to fabricate MnO/biocarbon

Table 1 Properties comparison of biomass-derived carbon/TMO composites in SCs

Electrode material	Electrolyte	S_{BET} / $(m^2 \cdot g^{-1})^a$	Potential window / V	Specific capacitance	Energy density	Power density	Cyclic stability	Refs.
Porous carbon microscale (MnO_2)	1.0 $mol \cdot L^{-1}$ Na_2SO_4	936	0–2.0	295 $F \cdot g^{-1}$ at 1 $A \cdot g^{-1}$	46.1 $Wh \cdot Kg^{-1}$	1.0 $kW \cdot kg^{-1}$	91% capacitance retention after 10000 cycles at 1.0 $A \cdot g^{-1}$	[74]
MnO_2 /hemp-derived activated carbon	1.0 $mol \cdot L^{-1}$ Na_2SO_4	438	0–2.0	340 $F \cdot g^{-1}$ at 1 $A \cdot g^{-1}$	33.3 $Wh \cdot Kg^{-1}$	14.8 $kW \cdot kg^{-1}$	98% capacitance retention after 3000 cycles at 1 $A \cdot g^{-1}$	[76]
MnO_2@bamboo leaf	1.0 $mol \cdot L^{-1}$ Na_2SO_4	–	0–1.6	76 $F \cdot g^{-1}$ at 0.5 $A \cdot g^{-1}$	11.47 $Wh \cdot Kg^{-1}$	1600 $W \cdot kg^{-1}$	85.3% capacitance retention after 1500 cycles at 0.5 $A \cdot g^{-1}$	[77]
BPC/MnO_2	1.0 $mol \cdot L^{-1}$ Na_2SO_4	325.1	0–1.8	384.9 $F \cdot g^{-1}$ at 0.5 $A \cdot g^{-1}$	34.2 $Wh \cdot Kg^{-1}$	9.58 $kW \cdot kg^{-1}$	90.7% capacitance retention after 5000 cycles	[78]
ACEP@δ-MnO_2	1.0 $mol \cdot L^{-1}$ Na_2SO_4	116.7	0–2.0	345.1 $F \cdot g^{-1}$ at 0.5 $A \cdot g^{-1}$	31.0 $Wh \cdot Kg^{-1}$	500 $W \cdot kg^{-1}$	92.8% capacitance retention after 5000 cycles at 0.5 $A \cdot g^{-1}$	[79]
RCFs/MnO_2/PEDOT	1.0 $mol \cdot L^{-1}$ Na_2SO_4	101.7	0–1.0	922 $F \cdot g^{-1}$ at 1 $A \cdot g^{-1}$	19.17 $Wh \cdot Kg^{-1}$	500 $W \cdot kg^{-1}$	83% capacitance retention after 10000 cycles	[80]
Hierarchically porous carbon-MnO-0.03	6.0 $mol \cdot L^{-1}$ KOH	930	0–1.6	162.7 $F \cdot g^{-1}$ at 0.5 $A \cdot g^{-1}$	57.7 $Wh \cdot Kg^{-1}$	400 $W \cdot kg^{-1}$	93.5% capacitance retention after 5000 cycles at 2 $A \cdot g^{-1}$	[81]
MnO/BPC	3.0 $mol \cdot L^{-1}$ KOH	133	0–1.6	637 $F \cdot g^{-1}$ at 3 $A \cdot g^{-1}$	35.9 $Wh \cdot Kg^{-1}$	800 $W \cdot kg^{-1}$	87% capacitance retention after 5000 cycles	[82]
Co_3O_4@meshy biomass carbon	6.0 $mol \cdot L^{-1}$ KOH	568.62	0–1.4	1212.4 $F \cdot g^{-1}$ at 0.5 $A \cdot g^{-1}$	59.82 $Wh \cdot Kg^{-1}$	700 $W \cdot kg^{-1}$	99.5% capacitance retention after 2000 cycles	[86]
CNFs/Co_3O_4	3.0 $mol \cdot L^{-1}$ KOH	413.4	0–1.6	785 $F \cdot g^{-1}$ at 0.5 $A \cdot g^{-1}$	13 $Wh \cdot Kg^{-1}$	257 $W \cdot kg^{-1}$	85.9% capacitance retention after 10000 cycles	[87]
L-Co_3O_4	6.0 $mol \cdot L^{-1}$ KOH	3151.2	0–1.6	1405.3 $F \cdot g^{-1}$ at 1 $A \cdot g^{-1}$	23.1 $Wh \cdot Kg^{-1}$	3990.6 $W \cdot kg^{-1}$	80.2% capacitance retention after 5000 cycles	[88]
Co_3O_4 NS@NOPC-200	2.0 $mol \cdot L^{-1}$ KOH	370	0–1.5	659.7 $F \cdot g^{-1}$ at 10 $mV \cdot s^{-1}$	42.5 $Wh \cdot Kg^{-1}$	746 $W \cdot kg^{-1}$	87.1% capacitance retention after 3000 cycles	[89]
NiO@PC	2.0 $mol \cdot L^{-1}$ KOH	379.5	0–1.5	849 $F \cdot g^{-1}$ at 1 $A \cdot g^{-1}$	–	–	92% capacitance retention after 8000 cycles	[93]
NiO/biochar	1.0 $mol \cdot L^{-1}$ KOH	198	0–1.2	1058 $F \cdot g^{-1}$ at 0.5 $A \cdot g^{-1}$	81 $Wh \cdot Kg^{-1}$	6 $kW \cdot kg^{-1}$	91% capacitance retention after 1500 cycles	[94]
$NiCo_2O_4$/GCNF	6.0 $mol \cdot L^{-1}$ KOH	–	0–1.5	1416 $F \cdot g^{-1}$ at 1 $A \cdot g^{-1}$	48.6 $Wh \cdot Kg^{-1}$	749.3 $W \cdot kg^{-1}$	88.5% capacitance retention after 10000 cycles	[99]
$NiCo_2O_4$ NSs@PD-PC	6.0 $mol \cdot L^{-1}$ KOH	143.21	0–1.6	922.9 $C \cdot g^{-1}$ at 1 $A \cdot g^{-1}$	39.1 $Wh \cdot Kg^{-1}$	799.9 $W \cdot kg^{-1}$	95.5% capacitance retention after 5000 cycles	[100]
BPC/Fe_2O_3	3.0 $mol \cdot L^{-1}$ KOH	775.8	0–1.6	987.9 $F \cdot g^{-1}$ at 1 $A \cdot g^{-1}$	96.7 $Wh \cdot Kg^{-1}$	20.65 $kW \cdot kg^{-1}$	76.2% capacitance retention after 5000 cycles	[105]

Table 1 continued

Electrode material	Electrolyte	S_{BET} / $(m^2 \cdot g^{-1})^a$	Potential window / V	Specific capacitance	Energy density	Power density	Cyclic stability	Refs.
$MnFe_2O_4$-NiS-PC	3.0 $mol \cdot L^{-1}$ KOH	1412	0–1.5	640 $F \cdot g^{-1}$ at 1 $A \cdot g^{-1}$	113 $Wh \cdot Kg^{-1}$	1500 $W \cdot kg^{-1}$	98% capacitance retention after 5000 cycles	[107]

a BET: Brunner–emmet–teller measurements

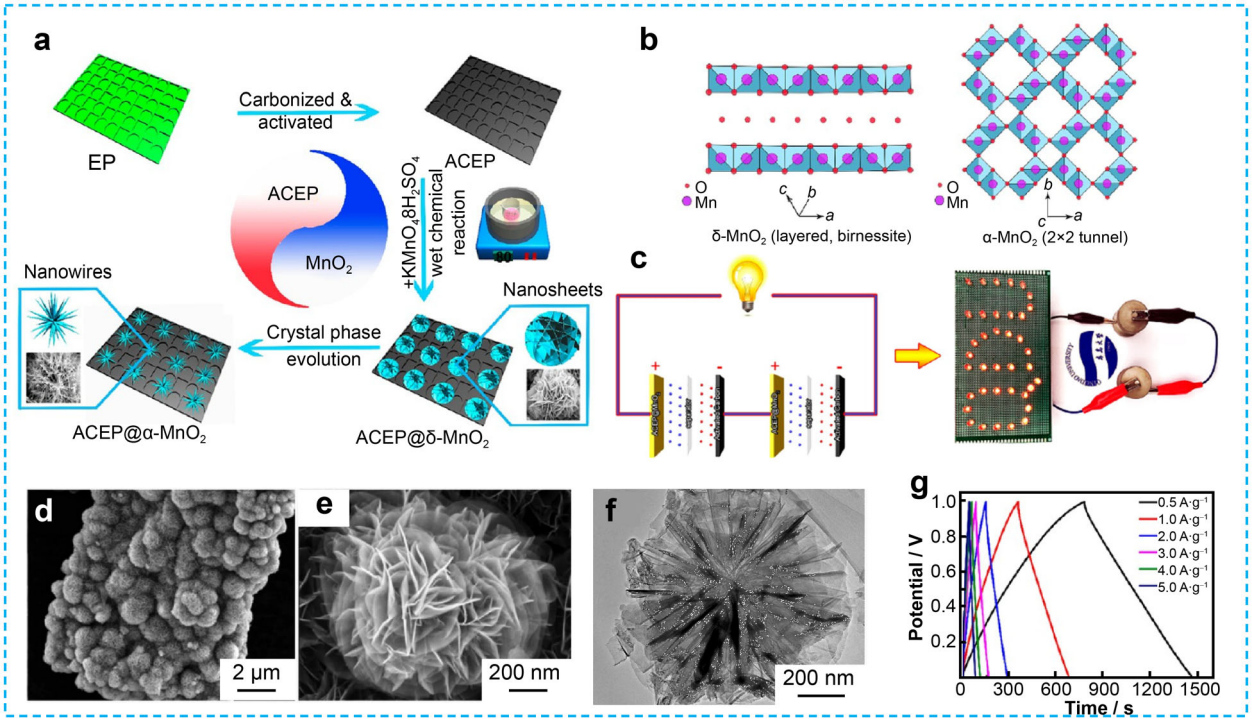

Fig. 1 Synthesis of ACEP@MnO_2 composites and their electrochemical performance: **a** synthesis of ACEP and ACEP@MnO_2; **b** crystal structure images of δ-MnO_2 and α-MnO_2; **c**, **g** electrochemical behavior of AC//ACEP@δ-MnO_2 asymmetric SC; **d**–**f** SEM and TEM images of ACEP@δ-MnO_2. Reproduced with permission from Ref. [79]. Copyright 2018, American Chemical Society

composites [81]. A nanostructure composite MnO/biomass-derived porous carbon (MnO/BPC) has been prepared by a simple immersion and calcination using natural agaric [82]. Interestingly, the MnO/BPC presented novel agaric-derived hybrid nanostructures, and MnO nanoparticles were encapsuled into porous carbon and deposited on carbon layer through chitin hydrogels and cellulose outershell as substrate to effectively resolve the problem of uniform distribution (Fig. 3a–g). The sample had high specific surface area and efficient electrical conduction. The MnO/BPC was further employed as a positive electrode and AC as negative electrode to fabricate assembled asymmetric supercapacitor that reached a high capacitance retention of 87% after 5000 cycles and high specific-energy of 35.9 $Wh \cdot kg^{-1}$ at 800 $W \cdot kg^{-1}$ (Fig. 3h–j).

4.2 Biomass-derived carbon/nickel-cobalt oxide composites

In transition metal oxides, binary Co_3O_4, NiO and ternary $NiCo_2O_4$ nanocomposites have been widely used in supercapacitors because of improved electrocatalytic ability and chemical stability. Moreover, the morphologies of transition metal oxides, such as nanoparticles, nanowires, nanosheet, hierarchical flowers, greatly have influence on the performance of electrode material [83–87]. Furthermore, the morphologies of functionalized carbons are also the key factor in electrochemical performance. Du et al. introduced three activated carbons (AC) with different morphologies derived from carbonization of rosewood (R), corncob (C), and lotus seedpod (L) waste plant body, and

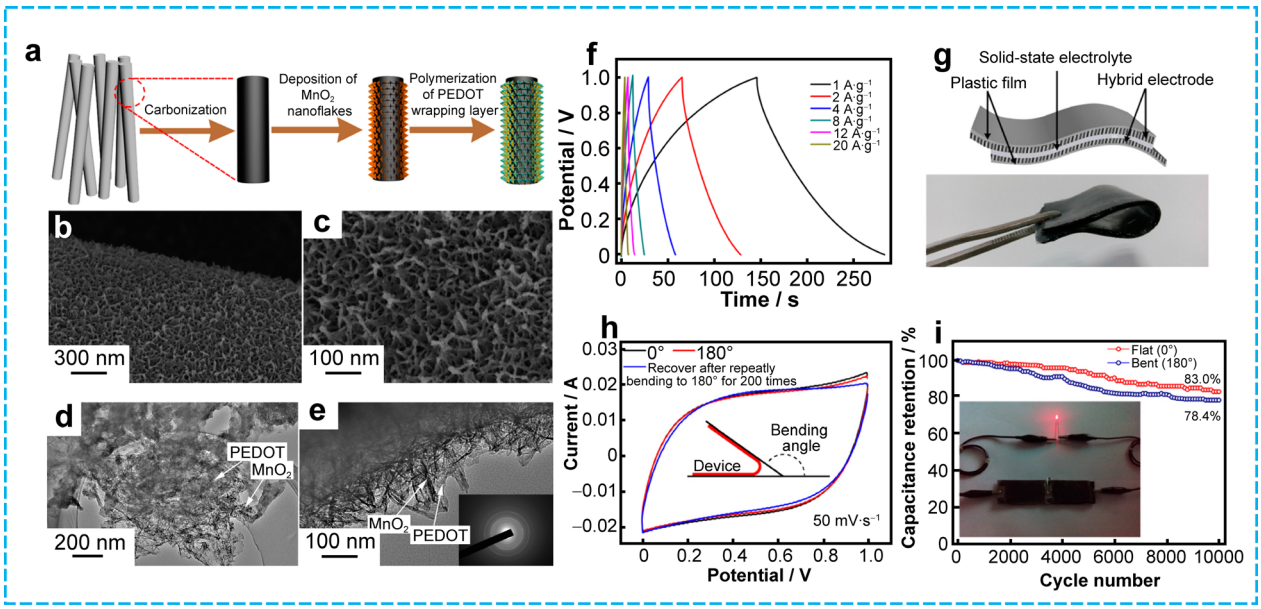

Fig. 2 Synthesis routes of RCFs/MnO_2/PEDOT hybrid electrode and their electrochemical performance: **a** synthesis process of hybrid electrode; **b**, **c** SEM images and **d**, **e** TEM images of RCFs/MnO_2/PEDOT; **f** GCD plots at different current densities; **g** flexible hybrid electrode; **h** CV curves at 50 $mV{\cdot}s^{-1}$ for device under different bending states; **i** cycling stability of device under flat and bent states over 10000 cycles, and (inset) red LED powered by two devices in series. Reproduced with permission from Ref. [80]. Copyright 2016, American Chemical Society

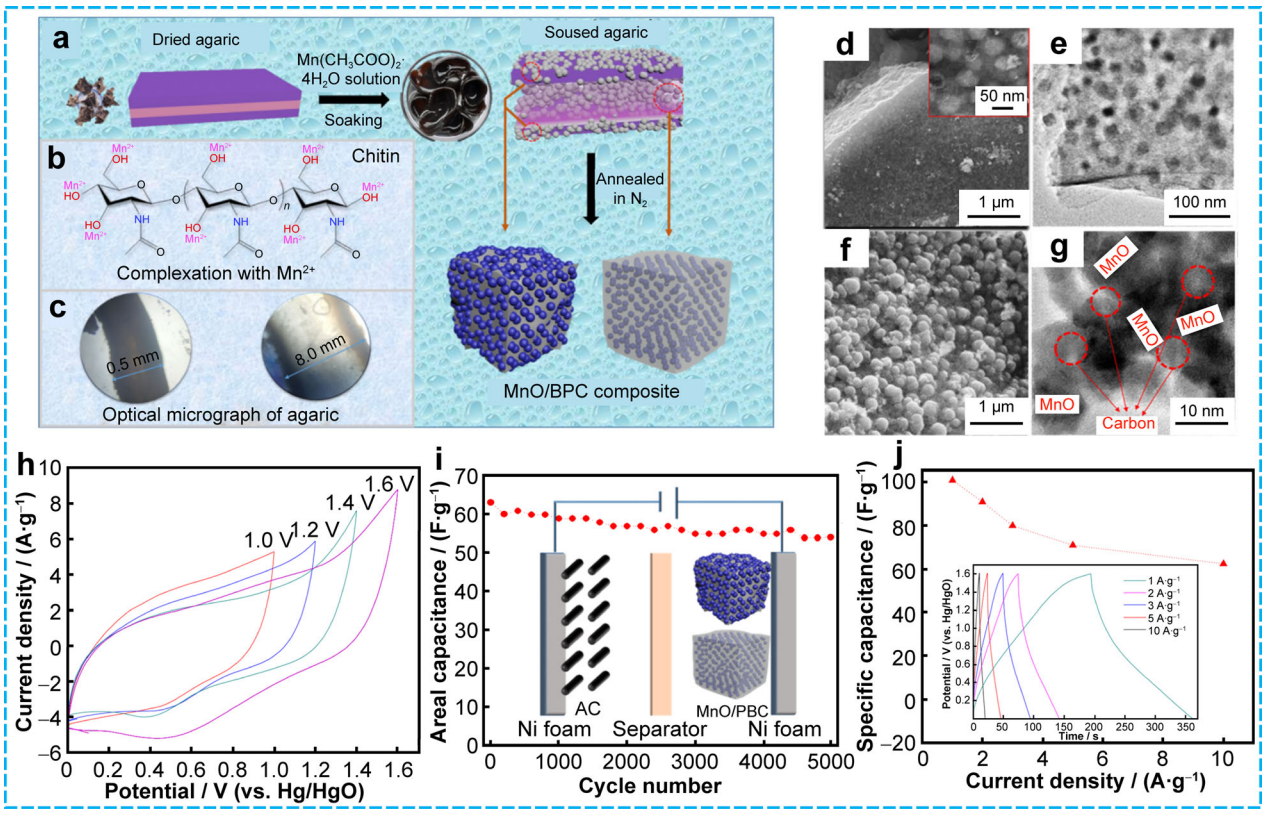

Fig. 3 Synthesis process of MnO/BPC derived natural agaric: **a** preparation procedure of MnO/BPC composite; **b** complexation between chitin and Mn^{2+} and **c** structure changes of agaric before and after immersed in Mn^{2+} solution; **d**, **f** SEM images and **e**, **g** TEM images of composites; **h** CV potential ranges of MnO/BPC//AC supercapacitor; **i** cycling stability and schematic graph of ASC device; **j** calculated capacitance of ASC in various current densities. Reproduced with permission from Ref. [82]. Copyright 2019, American Chemical Society

then bio-activated AC loaded Co_3O_4 nanoparticles via oxidation-precipitation and crystallization process (Fig. 4a–d) [88]. The result indicated L-AC from lotus seedpod decorated Co_3O_4 (L-Co_3O_4) presenting the best specific capacitance with 1405.3 $F{\cdot}g^{-1}$ at 5 $mV{\cdot}s^{-1}$ (Fig. 4e, f). The L-AC with interesting hollow tube morphology can afford porous channel to uniformly disperse the Co_3O_4 particles for promoting contact between ions and activation sites. Besides, according to report [89], Co_3O_4 nanosheets were anchored vertically on the surface of N, O, P-heteroatom doped porous carbon derived from the soybean dregs by hydrothermal route to obtain Co_3O_4 NS@NOPC composites (Fig. 5a, b). Interestingly, the lamellar Co_3O_4 in composites afford high energy density and high efficiency of charge transfer, in the meanwhile, N, O, P multi-heteroatom doped porous carbon (NOPC) can reduce the electrical resistance to improve the conductivity. Finally, solid state SCs based on Co_3O_4 NS@NOPC showed excellent electrochemical performance of up to 42.5 $Wh{\cdot}kg^{-1}$ at a power density of 746 $W{\cdot}kg^{-1}$ (Fig. 5c).

NiO-based composites with faradaic pseudocapacitive have also attracted lots of attention due to their application in electrochemical energy storage [90–93]. When electrode materials have the high surface area and a hierarchical structure to construct porous network, the faradic mechanism may be increased. In addition, NiO is deposited in porous thin film to produce active sites to enhance the faradic mechanism. Paravannoor [94] reported cellulose derived biochar wrapped Ni/NiO nanobrick composites (NiO/biochar) as a thin film pseudocapacitor electrode by a one-pot synthesis combustion synthesis (Fig. 6a). The brick NiO nanostructures possessed less grain boundaries compared to spherical structure, resulting in better charge mobility (Fig. 6b–d). And the specific capacitance value of the sample was up to 1058 $F{\cdot}g^{-1}$ with energy density of 81 $Wh{\cdot}kg^{-1}$.

Up to now, Co, Ni-based binary transition metal oxides have been widely studied as new electrode materials because of higher theoretical capacity (>2000 $F{\cdot}g^{-1}$), better electrical conductivity and lower diffusion resistance compared to single metal oxides [95–98]. $NiCo_2O_4$ with spinel structure can be obtained from Co_3O_4 in which Co atom was replaced by the Ni atom. For instance, nanoflower-like $NiCo_2O_4$ is anchored on the gelatin-derived porous carbon nickel foam (GCNF) through HTC method to produce binder-free $NiCo_2O_4$/GCNF composites for SCs [99]. GCNF provided mechanical substrate and current conductor without the binder, the resulting electrode showed a high specific capacitance of 1416 $F{\cdot}g^{-1}$ at 1 $A{\cdot}g^{-1}$, and $NiCo_2O_4$/GCNF//AC exhibited a high energy density of 48.6 $Wh{\cdot}kg^{-1}$ at a power density of 749.3 $W{\cdot}kg^{-1}$ and maintained 88.5% capacitance after 10,000 cycles at 1 $A{\cdot}g^{-1}$. Zhang's group used polydopamine-derived carbon microsheets wrapped ultrathin $NiCo_2O_4$ nanosheets ($NiCo_2O_4$ NSs) by in situ assembly process to fabricate shell-core sandwich composite $NiCo_2O_4$

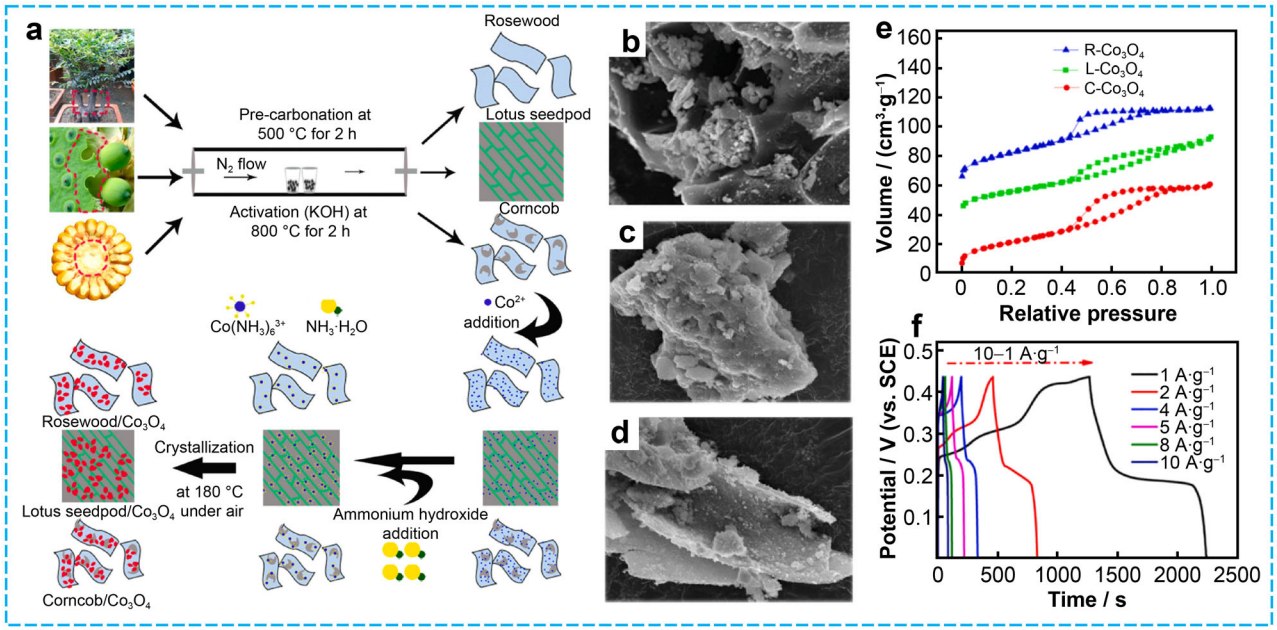

Fig. 4 Synthesis route and performance of biomass-derived activated carbons and their Co_3O_4 composites: **a** preparation of activated carbons AC-Co_3O_4 composites; **b–d** SEM images and **e** N_2 adsorption-desorption isotherms and plots of pore size distribution of AC-Co_3O_4 composites; **f** GCD curves of L-Co_3O_4 composite electrode. Reproduced with permission from Ref. [88]. Copyright 2022, Elsevier Ltd.

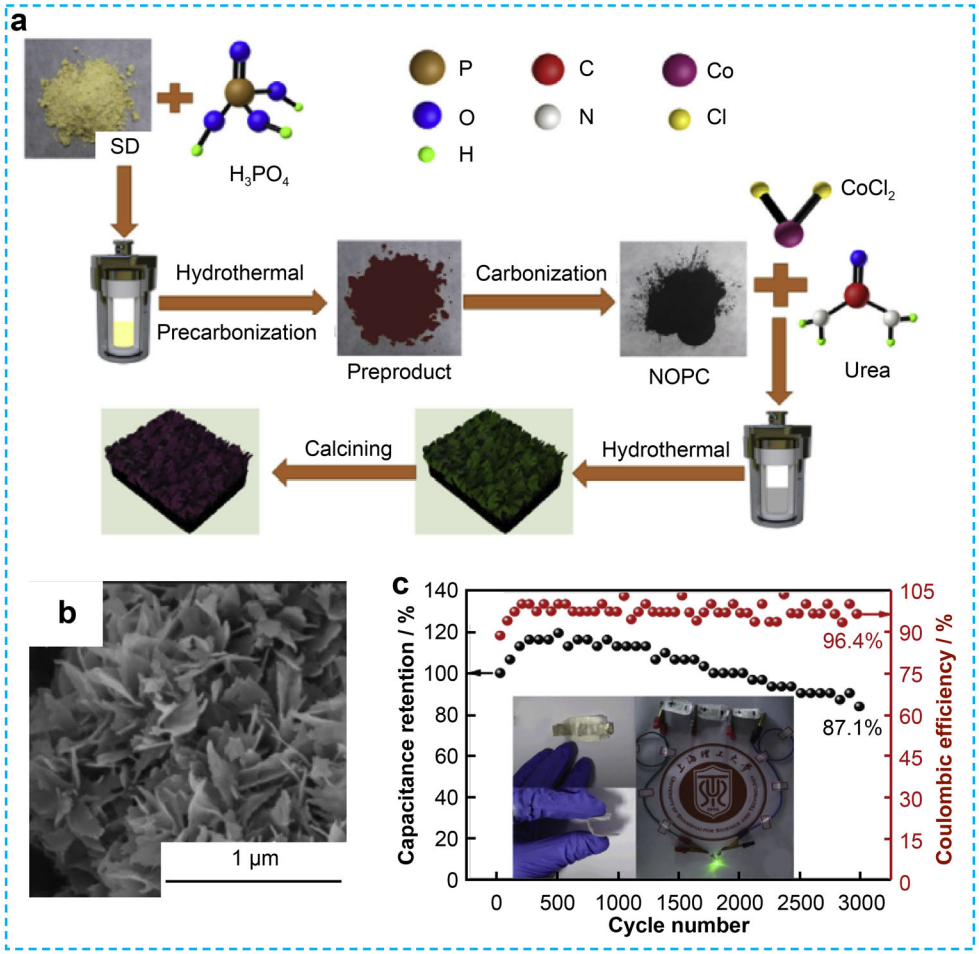

Fig. 5 Co_3O_4 NS@NOPC SC: **a** preparation process and **b** SEM image of composite materials; **c** stability performance of Co_3O_4 NS@NOPC based solid-state SC. Reproduced with permission from Ref. [89]. Copyright 2020, Elsevier Ltd.

NSs@PD-PC (PD-PC: polydopamine-modified poplar catkin carbon sheet) [100]. The combination between active $NiCo_2O_4$ and polydopamine-derived carbon could promote charge diffusion and ions conductivity for faradic redox reactions. The results indicated that $NiCo_2O_4$ NSs@PD-PC showed large specific capacitance and excellent cycling stability.

4.3 Biomass-derived carbon/iron oxide composites

Apart from the above metal-based porous carbon composites, iron oxide-based nanomaterials have been devoted in SCs due to the reversible faradaic reaction from Fe^{3+} to Fe^{2+} [101]. However, charge transports of Fe-based composites were limited because of their poor electrical conductivity. So far, many efforts were made to incorporate Fe oxide into carbon frameworks to construct hybrid structures for fast electron transfer channel [102–104]. For example, Fe_2O_3 ultrathin film was grown in the wheat-straw derived porous carbon to obtain BPC/Fe_2O_3 nanocomposites, that indicated an outstanding capacitance up to 987.9 $F{\cdot}g^{-1}$ at 1 $A{\cdot}g^{-1}$ and superior cycling performance with 82.6% retention after 3000 cycles [105]. Moreover, watermelon acted as the biomass carbon source to obtain a 3D porous carbonaceous gel (CGs) that was easy to be compressed and released. Then, Fe_3O_4 nanoparticles were evenly encapsulated into the network of GCs. After calcination, the specific capacitance of Fe_3O_4/biomass-derived porous carbon composites could be up to 333.1 $F{\cdot}g^{-1}$ at 1 $A{\cdot}g^{-1}$ and 96% capacitance retention after 1000 cycles could be obtained [106]. Compared to single oxide, the usage of more metal ions and porous carbon to construct novel electrode material is also an interesting work for SCs. Recently, Ghosh's group reported a $MnFe_2O_4$-NiS-porous carbon electrode material synthesized through an one-pot wet impregnation technique (Fig. 7a) [107], in which the porous carbon derived from coconut fiber with a high surface area of 1410 $m^2{\cdot}g^{-1}$. The $MnFe_2O_4$ nanoparticles could provide rich reaction sites and porous carbon could produce easy diffusion of

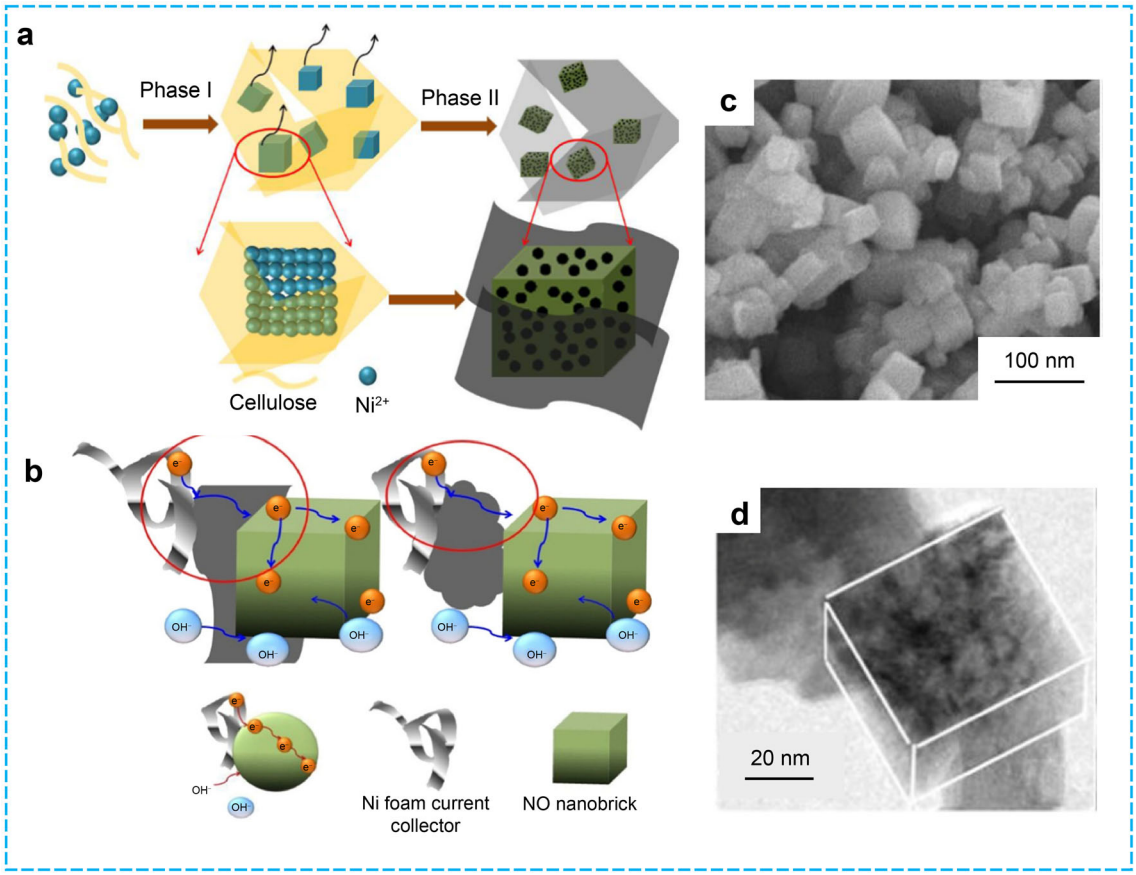

Fig. 6 NiO/biochar composites: **a** synthesis mechanism and **b** charge transfer mechanism NiO/biochar composite nanobricks; **c**, **d** SEM and TEM images of composite. Reproduced with permission from Ref. [94]. Copyright 2018, Elsevier Ltd.

electrolyte ions to increase mechanical stability (Fig. 7b, c). As a result, the synergy effect of $MnFe_2O_4$ and NiS nanoparticles embedded in biomass-derived porous carbon to promote the ASC device ($MnFe_2O_4$-NiS-PC//PC) delivered a higher energy density of 113 $Wh{\cdot}kg^{-1}$ at a power density of 1500 $W{\cdot}kg^{-1}$, and only 2% capacitance deterioration under 10000 cycles (Fig. 7d, e). To sum up, the composites based on bimetallic oxide exhibit higher specific capacitance than monometallic ones due to more redox processes and interaction in mix metal cations. At the same time, the metallic component is also an important factor to affect supercapacitors performance. On the other hand, the synergetic effect between metal ions and biomass-derived carbonaceous materials is also an important factor to determine morphologies, conductivity, surface area and pore distribution of electrode materials.

5 Biomass-derived carbon/TMS composites

TMS exhibits better electrical performance due to the lower electronegativity and more valence states as a new type of electrode material. However, the poor capacity retention, large volume variation, sluggish reaction kinetics, and stability are great obstacles to TMS electrochemical application [108]. In general, the pure TMS materials also face the problems of agglomeration and poor electrical conductivity. To solve the above shortcomings, an effective way is the mixture of carbonaceous materials and TMS. According to Chen group's report, the broussonetia papyrifera branches-derived N-doped carbon dot (NCD) regulated the porous hollow NiCoS to gain NCD/NiCoS composite via water bath and hydrothermal reaction (Fig. 8a–c) [109]. Interestingly, the morphology transforms of NCD/NiCoS were ascribed to anion exchange during the sulfidation. Subsequently, the optimized sample was fabricated a hybrid supercapacitor to gain high power density and energy densities and kept 96.5% capacitance after 10000 cycles (Fig. 8d). Later, hierarchical microspheres ZnCoS nanosheets have also been deposited directly biomass derived hydrothermal carbon spheres (HTCSs) via water-based binder-free hydrothermal method [110]. The obtained Zn-Co-S@HTCSs as positive electrode and core/shell-like Fe_2O_3 decorated polyaniline (PANI) nanotubes as negative electrode to construct ASCs device displayed a remarkable energy density of 85 $Wh{\cdot}kg^{-1}$ at a power

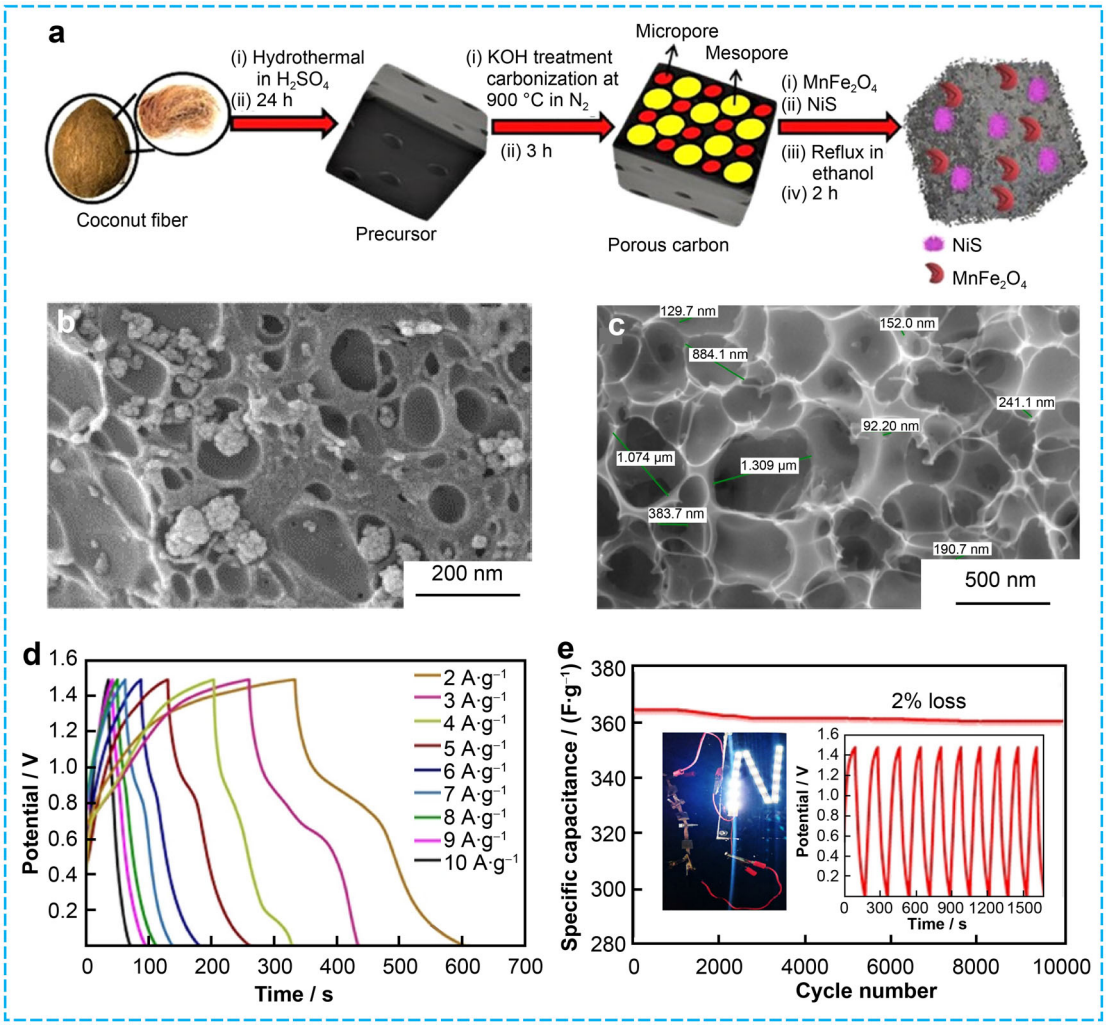

Fig. 7 Synthesis and performance of $MnFe_2O_4$-NiS-porous carbon electrode material: **a** synthesis of $MnFe_2O_4$-NiS-PC nanocomposite; **b** SEM image of a 3D porous network derived from coconut fiber; **c** SEM image of $MnFe_2O_4$-NiS-PC nanocomposite; **d** GCD and **e** cycling stability test of composite electrode materials. Reproduced with permission from Ref. [107]. Copyright 2021, American Chemical Society

density of 460 $W \cdot kg^{-1}$ with a broad potential window. In all, the flexible biomass-derived carbons as substrates not only supply porous structure for electrolyte transfer, but also offer more active sites for uniform disperse TMO/TMS nanoparticles through hydrothermal reaction or electrochemical deposition. Compared to TMO, the sulfur atom shows lower electronegativity than oxygen, that is benefit for production of flexible phase to promote the electron transfer and electrochemical performances. In addition, TMS can easily exhibit layered structures by van der Waals forces containing three atom layers (S-M-S), resulting in higher electrical double layer capacitance. Simultaneously, the intercalation activity in conversion process can generate higher specific capacitance and poor cycling performance. The obstacles of the electrochemical applications of TMS are low electrical conductivity and volume change during cycling. Furthermore, the composites synthesized by TMS and carbon materials could occur structural damage in the electrochemical processes causing fast capacitance fading. Thus, we need continue to further study the synergetic effects between TMS and biomass-derived carbon to offset their respective drawbacks and promote the application of supercapacitor for biomass-derived carbon/TMS composites.

6 Biomass-derived carbon/LDH composites

LDH, also known as a hydrotalcite-like compound, is one of the most widely applied homogeneous and mixed metal hydroxides showing lamellar structure with a chemical formula of $[M(II)_{1-x}M(III)_x(OH)_2]^{x+}[X^{m-}_{x/m} \cdot nH_2O]^{x-}$, in which M(II) is a divalent cation (e.g., Fe, Ni, Mn, Zn, Cu) and M(III) is a trivalent metal cation (e.g., Fe, Al, Co, Cr,

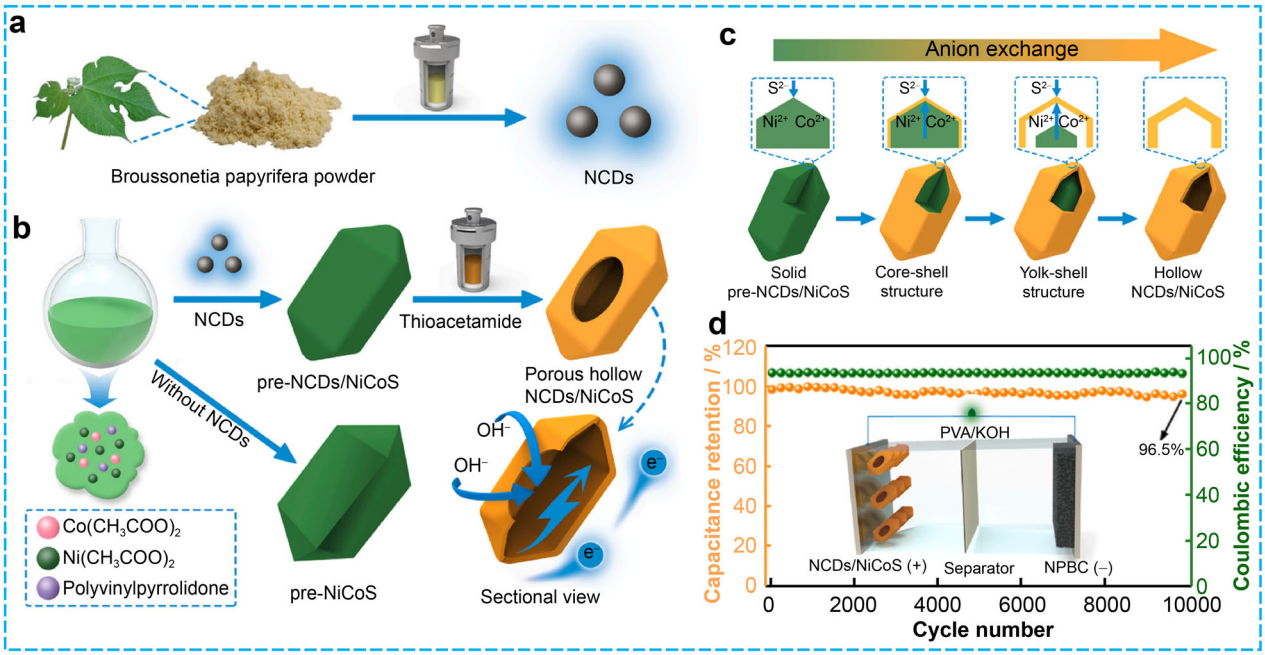

Fig. 8 NCDs/NiCoS composites from **a**–**c** preparation of NCDs, NCDs/NiCoS nanocomposites and hollow structure; **d** illustration of NCDs/NiCoS//NPBC HSC device, cyclic performance and Coulombic efficiencies (where PVA is polyvinyl alcohol). Reproduced with permission from Ref. [109]. Copyright 2021, Elsevier Ltd.

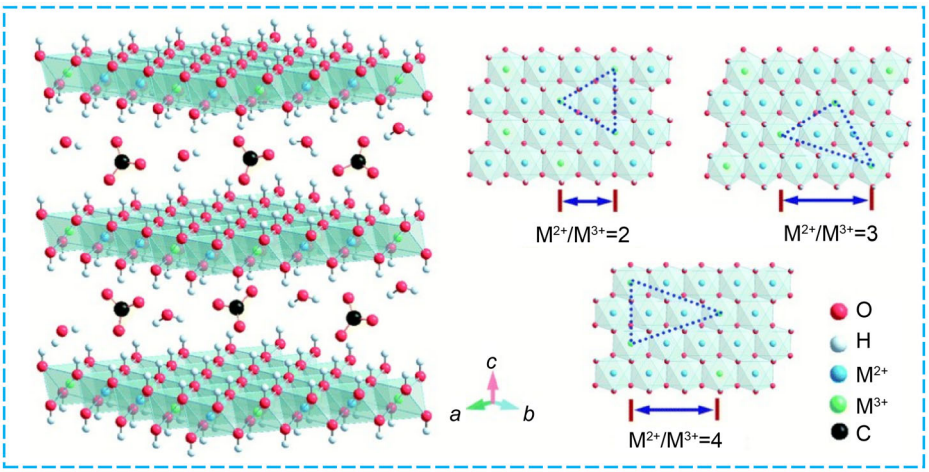

Scheme 3 Structure of carbonate-intercalated LDHs with different M^{2+}/M^{3+} molar ratios. Reproduced with permission from Ref. [111]. Copyright 2014, Royal Society of Chemistry

Ga) and X^{m-} is the interlayer anion (e.g., CO_3^{2-}, NO_3^-) (Scheme 3) [111]. In the asymmetry LDH crystals, cations are present in the layered sheet of crystal and anions existed in the interlayer. The easy adjustment of the cations in the layered sheet and the exchangeability of anions in the interlayer can afford them intriguing electrochemical activities. Therefore, plenty of reports have been studied about the application of LDH in supercapacitors, such as CoNi-LDH, NiAl-LDH, CoAl-LDH, NiMn-LDH, CoFe-LDH, and NiFe-LDH [112–121], where the exhibited excellent pseudocapacitance behavior could guarantee its wide applications as high performance electrochemical devices [122–128]. However, it should not be ignored that the capacities of pure LDH are restricted by the poor active sites, the accumulation of metal nanoparticles and volume expansion during charge-discharge cycles. Meantime, LDH materials could suffer from the charge transfer process on the surface and the weak electrical conductivity because of the limited redox kinetics, resulting in unsatisfactory electrochemical performance compared to other metal-

based materials. Thus, to address these issues and maximize the advantages of LDH, combining LDH with biomass-derived carbonaceous materials (activated carbon, graphene, porous carbon, carbon nanotubes, carbon aerogels) can be considered as an effective pathway. Due to high specific surface areas and excellent conductivity, biomass-derived carbon materials not only provide adequate space for depositing LDH to maximize electroactive areas, but also improve charge transfer and redox reaction kinetics, resulting in high capacity and energy density. Moreover, the rough structures from biomass-derived carbon can withstand the mechanical pressure of faradaic reactions in the charging and discharging process, and is beneficial to prolong the cycle life of pseudocapacitive materials. As a consequence, many kinds of carbons derived from biomass have been chosen and incorporated into LDH to improve their electrochemical properties as pseudocapacitive composites [129].

Golmohammadi and Amiri [130] reported an electroactive composite (NiAl-LDH@KP-GO) based on biomass derived 3D graphene oxide (GO) and Karrapo (KP) as biomass source mixed with NiAl-LDH, in which the graphene could act as an anchoring site for the nucleation and growth of LDH to successfully solve the problem of accumulation and aggregation between graphene and LDH (Fig. 9a, b). As used in supercapacitor, NiAl-LDH@KP-GO showed a specific capacitance of 1390 $F \cdot g^{-1}$ at 1 $A \cdot g^{-1}$, superior to NiAl-LDH and NiAl-LDH@GO. An asymmetric device was assembled, exhibiting a high energy density of 173 $Wh \cdot kg^{-1}$ and the power density of 28.8 $kW \cdot kg^{-1}$ with excellent cycling stability of 92% after 5000 cycles (Fig. 9c, d). In another example, Tan et al. obtained flower-like CAS@NiMn-LDH composites supported by honeycomb-like porous carbon from the chingma abutilon seed (CAS) as the precursor [131]. Firstly, the honeycomb-like porous carbon has been synthesized by KOH-activated treatment, and more porous structures and high surface afford plentiful active sites to adsorb metal ions and transport ions. Secondly, the NiMn-LDH nanosheets were closely adhered to the backbone of CAS by a facile hydrothermal treatment (Fig. 10a). In the process, the highly conductive porous carbon provided a skeleton to prevent the accumulation of NiMn-LDH microspheres and more exposed active sites reduced

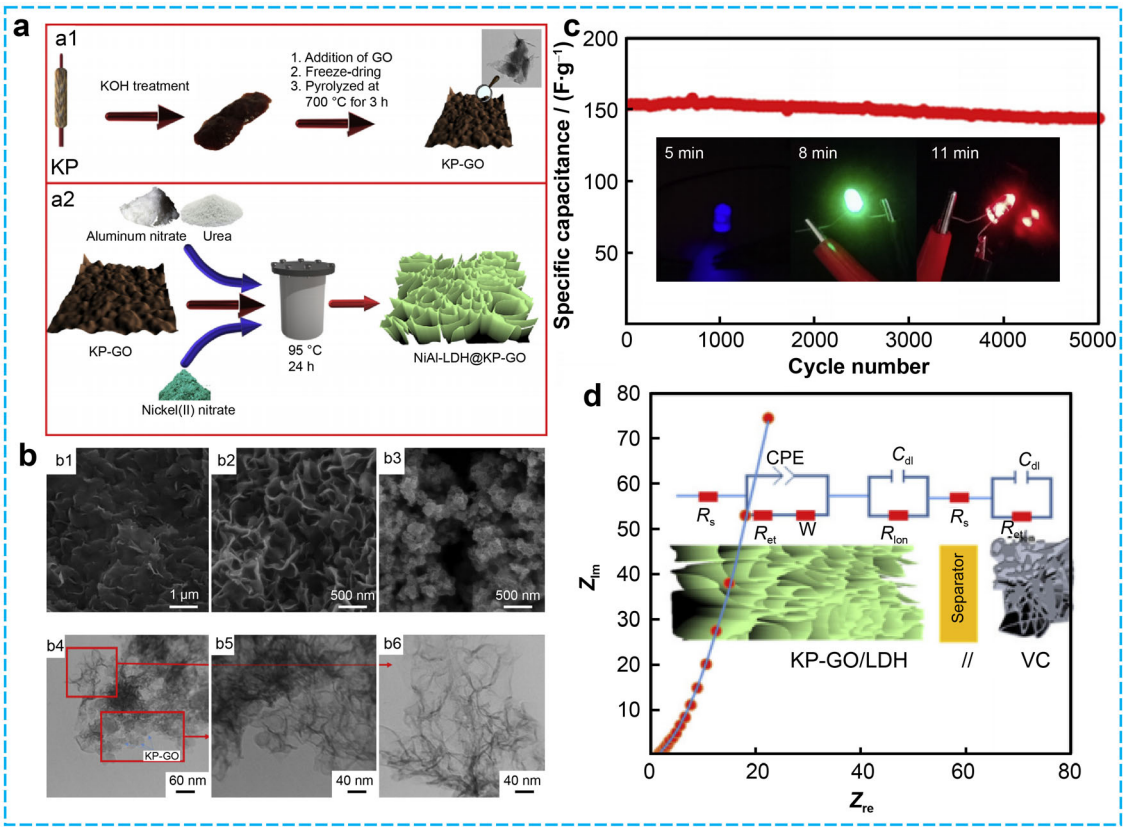

Fig. 9 Composite NiAl-LDH@KP-GO: **a** preparation steps of NiAl-LDH@KP-GO; **b** SEM and TEM images of NiAl-LDH, NiAl-LDH@GO and NiAl-LDH@KP-GO; **c** cycling stability of NiAl-LDH@KP-GO//VC device (VC: Vulcan XC-72R carbon) and photograph lighting an light emitting diode (LED) screen; **d** Nyquist plot of NiAl-LDH@KP-GO//VC device (Z_{im}: imaginary axis; Z_{re}: real axis; R_s: solution resistance of electrolyte; R_{et}: charge-transfer resistance; R_{ion}: resistance of ionic conductive liquid phase; C_{dl}: double-layer capacitance; CPE: constant phase angle element). Reproduced with permission from Ref. [130]. Copyright 2020, Elsevier Ltd.

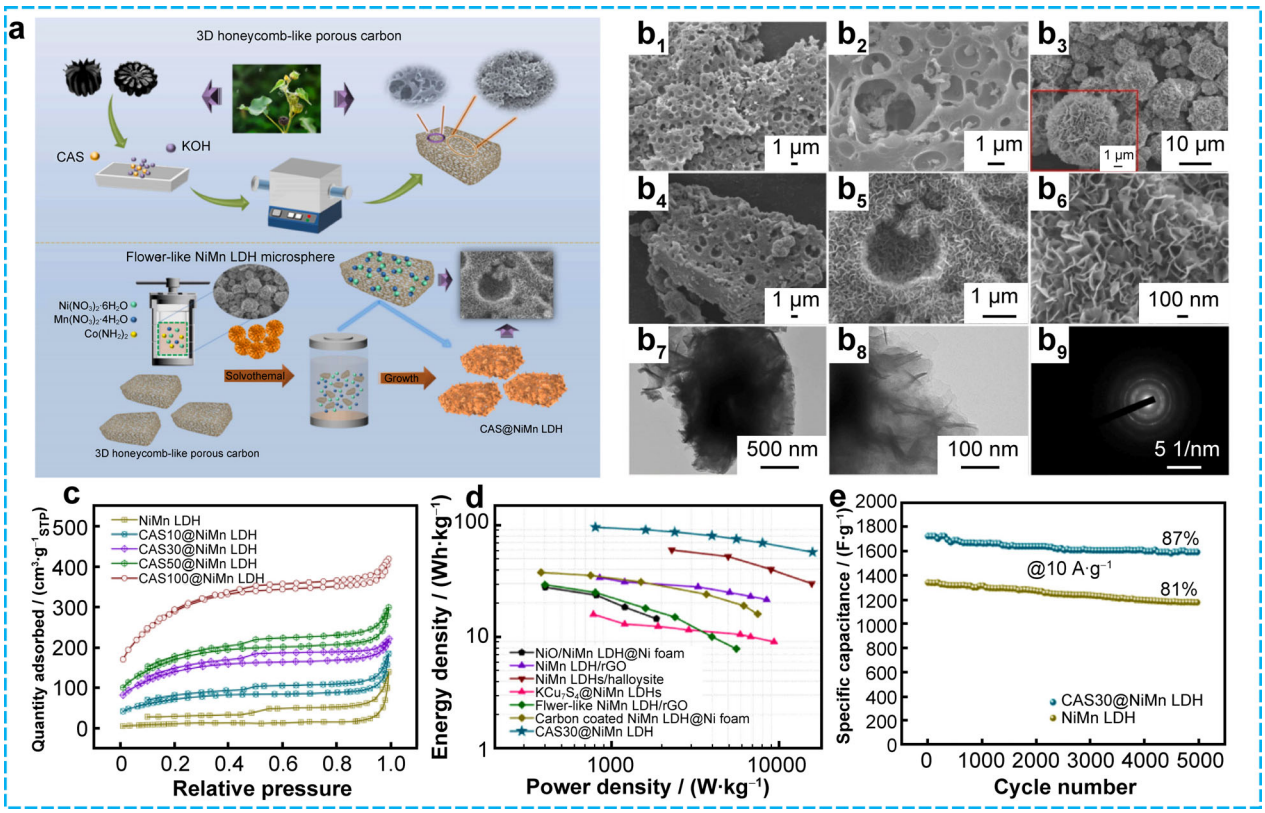

Fig. 10 Flower-like CAS@NiMn-LDH composites: **a** preparation of CAS-based honeycomb-like porous carbon and CAS@NiMn-LDH; $\mathbf{b_1}$–$\mathbf{b_6}$ SEM images and $\mathbf{b_7}$–$\mathbf{b_9}$ TEM images of porous carbon, NiMn-LDH and CAS@NiMn-LDH; **c** N_2 adsorption-desorption isotherms of CAS@NiMn-LDH (CAS10@NiMn-LDH, CAS30@NiMn-LDH, CAS50@NiMn-LDH, CAS100@NiMn-LDH, corresponding to the various CAS contents); **d** Ragone plots and **e** cycling performance of CAS@NiMn-LDH. Reproduced with permission from Ref. [131]. Copyright 2021, Elsevier Ltd.

electron transport impedance, promoting the pseudocapacitive performance (Fig. 10b). Finally, the optimal CAS30@NiMn-LDH showed a high specific capacity of 1719 $F{\cdot}g^{-1}$ at 1 $A{\cdot}g^{-1}$, and the maximum energy density of 95.29 $Wh{\cdot}kg^{-1}$ at 802 $W{\cdot}kg^{-1}$ was observed by the as-assembled device, indicating excited cycle performance (87% retention after 5000 cycles) (Fig. 10c–e).

More importantly, the effective electrode materials mainly depend on flexible substrates to keep good mechanical elasticity and high electrical conductivity [132]. Among numerous biomass materials, bacterial cellulose (BC)-based materials can be used for the preparation of electrode materials due to high flexibility, biocompatibility, high tensile strength, and low-cost. In supercapacitor electrodes, the unique nanofibrous structure of BC are beneficial to enlarge the active volume of electrodes for energy storage devices. Moreover, nanostructured LDHs depositing on BC-based material as flexible and conductive substrate can maximize their potential [133, 134]. Therefore, many efforts have been devoted on BC-derived carbon materials coupling with LDH to fabricate as flexible electrodes in supercapacitors [135–139]. However, the drawback of these composites is the incompatibility between inactive surface of substrate and inorganic materials. To solve this problem, Cheng's group reported a novel highly flexible, foldable and stretchable NiCo-LDH/PANI/BC electrode material [140]. Firstly, BC shows a unique 3D network after being freeze-dried as a template, then the in situ coating PANI on BC retains the 3D open network to afford more active sites for loading NiCo-LDH, meanwhile PANI layer acts as a "nanoglue" to anchor NiCo-LDH nanoparticles due to its hydrophilicity and rough surface (Fig. 11a). The ternary composites NiCo-LDH/PANI/BC show excellent flexibility and electrochemical performance with a high specific capacitance of 1690 $F{\cdot}g^{-1}$ at 1 $A{\cdot}g^{-1}$, higher than that of PANI/BC and NiCo-LDH/BC. In addition, the obtained composites were assembled with N-doped carbonized BC/carbon cloth as a flexible all-solid-state asymmetric supercapacitor (ASC) generating a high energy density of 47.3 $Wh{\cdot}kg^{-1}$ at the power density of 828.9 $W{\cdot}kg^{-1}$ (Fig. 11b). Another similar example is BC nanofiber as scaffold depositing conjugated polypyrrole and NiMn-LDH by in situ layer-by-layer deposition

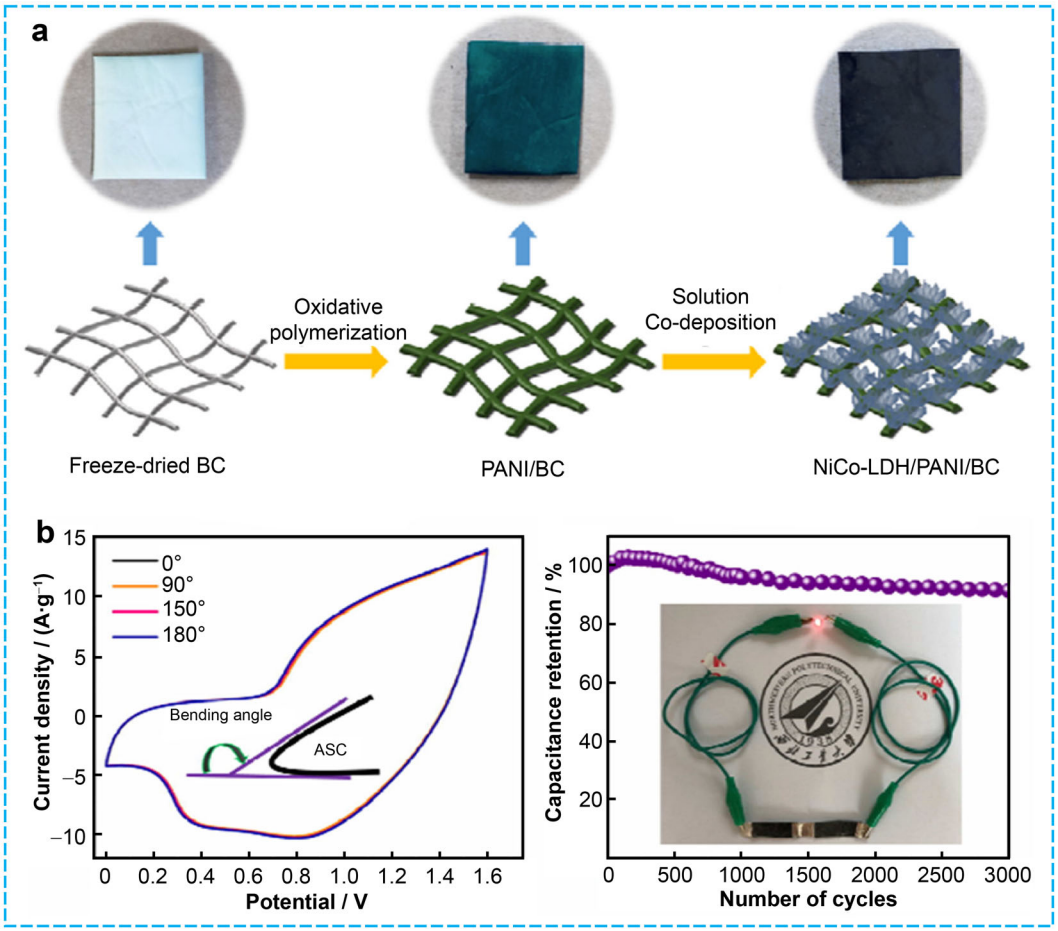

Fig. 11 NiCo-LDH/PANI/BC composites: **a** synthetic process of composites; **b** flexible ASC device bended with different angles and cycling performance of SCs. Reproduced with permission from Ref. [140]. Copyright 2018, Royal Society of Chemistry

method (NiMn-LDH/PPy/BC) for efficient supercapacitors [141].

Additionally, heteroatoms-doping, especially C, N, S-doping have received lots of attention due to more electron transfer channels and fast redox reactions of surface functional groups [142–147]. Interestingly, the C, N-doped novel nickel hydroxide composites (C/N-$Ni(OH)_2/Ni_xS_y$) were obtained by egg white as precursor giving rise to a particle/flake sandwich structure by a one-step hydrothermal method (Fig. 12a) [148], in which unique structure effectively inhibit the agglomeration of $Ni(OH)_2$ nanoflakes and Ni_xS_y nanoparticles to afford higher surface area (Fig. 12b). The heteroatoms-doping and well-preserved structure lead to outstanding 1731.2 $F{\cdot}g^{-1}$ at 0.5 $A{\cdot}g^{-1}$ (Fig. 12c). Meanwhile, the hybrid supercapacitor (C/N-$Ni(OH)_2/Ni_xS_y$//reduced graphene oxide hydrogel) exhibits an extremely long cycling life with 134.6% capacitance retention over 10000 cycles at 5 $A{\cdot}g^{-1}$ (Fig. 12d). The result manifests that heteroatoms-doping significantly promotes the electrical conductivity and supplies more active sites for the electrochemical performance.

In general, there are two methods to obtain the combination of biomass-derived carbon and LDH. The first way is self-assembly based on the strong electrostatic interactions between the positively charged surface of LDHs and the negatively charged surface of modified biomass-derived carbon to fabricate composites. The other situation is LDH can in situ grow on the biomass-derived carbon, which is employed as growth substrates. Specifically, the negatively charged surface of biomass-derived carbon can easily adsorb the metal cations in solution, then co-precipitation of metal cations occurs in the surface of carbon materials and gradually grows into various kinds of LDH. During this process, biomass-derived porous carbon materials provide large specific area to support the in situ growth of LDH [149]. The main capacitive properties of biomass-derived carbon/LDH composites are reported in Table 2.

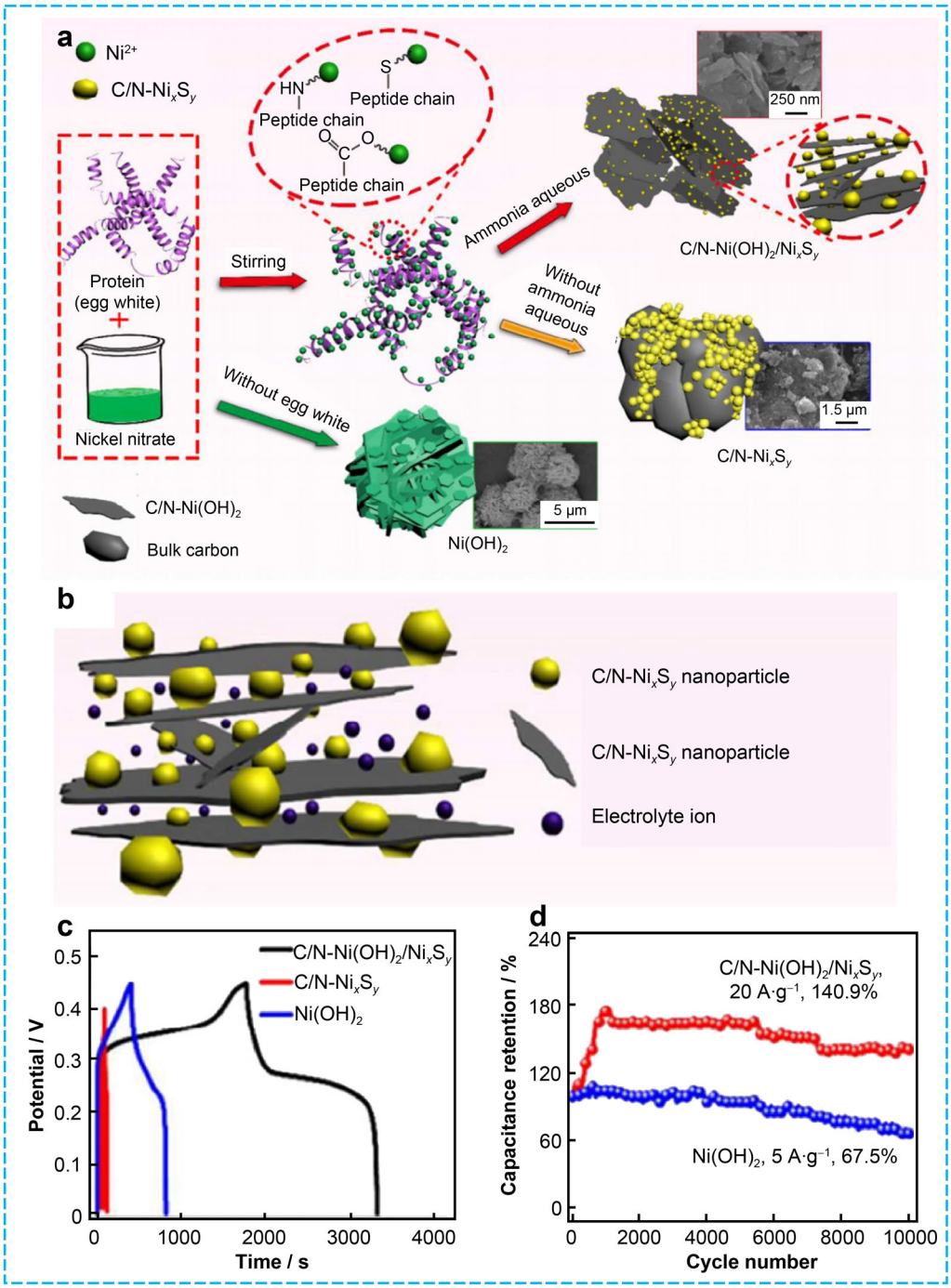

Fig. 12 C/N-Ni(OH)$_2$/Ni$_x$S$_y$ composites: **a** formation process of composites; **b** particle/flake structure for ions migration in composites; **c**, **d** GCD curves at a current density of 0.5 A·g^{-1} and cycling performance of composites. Reproduced with permission from Ref. [148]. Copyright 2018, Royal Society of Chemistry

7 Biomass-derived carbon/MOFs composites

In general, the electrochemical performance of electrode materials mainly depends on the surface, that is because the surface with higher energy can afford more reactivity, at the same time, the surface of electrode material also needs to decrease energy to maintain the stability via interaction with suitable matter from the outside environment. Nanoporous material can act as an effective electrochemical material because of boosting surface area for rich active sites and accessible inner structure for shortening electron diffusion path in electrolyte. Therefore, nanoporous

Table 2 Properties comparison of biomass-derived carbon/LDH and MOFs composites and their usage in SCs

Electrode material	Synthesis strategy	S_{BET} / ($m^2 \cdot g^{-1}$)	Potential window / V	Specific capacitance	Energy density	Power density	Cyclic stability	Refs.
NiAlLDH@KP-GO	One-step autoclave process	390	0.6–1.6	1390 $F \cdot g^{-1}$ at 1 $A \cdot g^{-1}$	173 $Wh \cdot kg^{-1}$	960 $W \cdot kg^{-1}$	5000 cycles with 94% capacitance retention	[130]
CAS30@NiMn LDH	KOH activation , HTC	476.52	0–1.6	1719 $F \cdot g^{-1}$ at 1 $A \cdot g^{-1}$	95.29 $Wh \cdot kg^{-1}$	802 $W \cdot kg^{-1}$	5000 cycles with 87% capacitance retention	[131]
NiCo-LDH/PANI/BC	Chemical bath deposition	–	0–1.6	1690 $F \cdot g^{-1}$ at 1 $A \cdot g^{-1}$	47.3 $Wh \cdot kg^{-1}$	828.9 $W \cdot kg^{-1}$	3000 cycles with 91.4% capacitance retention	[140]
NiMn-LDH/PPy/BC	Layered deposition	72.9	0–1.6	1427 $F \cdot g^{-1}$ at 1 $A \cdot g^{-1}$	29.8 $Wh \cdot kg^{-1}$	299.0 $W \cdot kg^{-1}$	2000 cycles with 80.5% capacitance retention	[141]
Carbonized bacterial cellulose-N@LDH	Layered deposition	405.8	0–1.6	1949.5 $F \cdot g^{-1}$ at 1 $A \cdot g^{-1}$	36.3 $Wh \cdot kg^{-1}$	800.2 $W \cdot kg^{-1}$	2500 cycles with 89.3% capacitance retention	[147]
C/N-$Ni(OH)_2$/Ni_xS_y	One-step hydrothermal method	101.3	0–1.6	1731.2 $F \cdot g^{-1}$ at 0.5 $A \cdot g^{-1}$	38.98 $Wh \cdot kg^{-1}$	404.36 $W \cdot kg^{-1}$	10000 cycles with 107.6% capacitance retention	[148]
Hierarchically porous nitrogen-doped carbon-950	Self-assembly, carbonization	1131	–1.6	134 $F \cdot g^{-1}$ at 1 $A \cdot g^{-1}$	23.75 $Wh \cdot kg^{-1}$	50 $W \cdot kg^{-1}$	5000 cycles with 81% capacitance retention	[160]
C@ZIF-67	Self-assembly, carbonization	174.7	0–1.5	1044.8 $F \cdot g^{-1}$ at 1 $A \cdot g^{-1}$	85.13 $Wh \cdot kg^{-1}$	750 $W \cdot kg^{-1}$	20000 cycles with 87% capacitance retention	[162]
NCNF2-900	Self-assembly, carbonization	391	0–1.0	211 $F \cdot g^{-1}$ at 1 $A \cdot g^{-1}$	5.7 $Wh \cdot kg^{-1}$	125 $W \cdot kg^{-1}$	5000 cycles with 91% capacitance retention	[163]
Hetero-fNCs	Self-assembly, carbonization	481.9	0–1.6	426.9 $F \cdot g^{-1}$ at 0.5 $A \cdot g^{-1}$	30 $Wh \cdot kg^{-1}$	1440 $W \cdot kg^{-1}$	5000 cycles with 89.5% capacitance retention	[164]
Ni_3S_2@Co_9S_8/N-HPC	Self-assembly, freeze-drying carbonization	360.1	0–1.6	1970.5 $F \cdot g^{-1}$ at 0.5 $A \cdot g^{-1}$	77.1 $Wh \cdot kg^{-1}$	263.3 $W \cdot kg^{-1}$	5000 cycles with 89.5% capacitance retention	[165]
WS@Ni-MOF/SPANI	Self-assembly, carbonization	9.5392	0–1.65	1722 $F \cdot g^{-1}$ at 1 $A \cdot g^{-1}$	34.79 $Wh \cdot kg^{-1}$	824 $W \cdot kg^{-1}$	20000 cycles with 89.5% capacitance retention	[169]

material is an excellent candidate as SCs to promote cycling stability and increase capacitance. Meanwhile, although biomass-derived carbon can promote discharge rate with long cycle life as supercapacitors, less energy density of carbon-base electrode materials is a key problem to solve in application [126, 150]. As a type of nanoporous material, MOFs are constructed by metal ions or cluster as node and organic ligand as linker, in which metal nodes can afford redox reaction centers and the organic linker can produce porous carbon as precursor. However, electrode materials derived from MOFs usually show poor mechanical strength and weak conductivity as electrode material compared with other carbon-based materials [151]. Additionally, the problem of aggregation of MOFs nanocrystals and the structural destruction in high temperature condition all greatly limit application in SCs [152]. To overcome this issue, the development of biomass-derived carbon/MOFs composites can make up for the defects of single MOFs,

improving electrochemical performance because of increased amounts of active components [153–156].

In biomass-derived carbon/MOFs composites, zeolitic-imidazole frameworks (ZIFs) have been reported as the most promising candidates to obtain high porous heteroatom-doped carbon networks for the performance of SCs due to high surface area, ordered pore structure, adjustable structure and simple synthesis method [157]. The most popular materials of ZIFs in SCs are ZIF-8 and ZIF-67, in which sodalite topology structure can provide the feasible condition for multi-structural derivatives, and the N-containing organic ligand can also create nanoporous carbon and other metal derivatives [158–161]. Simultaneously, Co and Ni metals in ZIFs not only promote the specific capacitance but also accelerate the ion and electron transfer in electrode. Li and coworkers manufactured a hierarchical composites materials with honeycomb-like carbon frameworks [162], the materials were prepared using waste straw as biomass template, $Ni(CH_3COO)_2$ as pore former and ZIF-67 by a string and annealing process (Fig. 13a). After carbonization, CoN_3 alloy particles generated from ZIF-67 were uniformly distributed on the surface of the biomass carbon skeleton, and the hierarchical carbon frameworks could hinder the aggregation of CoN_3 nanoparticles owing to the restrained space environment. The optimal composites C@ZIF-67-600 displayed a remarkable capacitance (1044.8 $F{\cdot}g^{-1}$ at 1 $A{\cdot}g^{-1}$), and the C@ZIF-67-600//AC device indicated a maximum density of 85.13 $Wh{\cdot}Kg^{-1}$ at a power density of 750 $W{\cdot}kg^{-1}$ and good cycling stability (87% capacitance maintenance after 20000 cycles at 5 $A{\cdot}g^{-1}$) (Fig. 13b).

Meanwhile, Chen's group [163] reported a 3D interconnected N-doped carbon nanofiber aerogels (NCNF) for the first time through in situ growth ZIF-8 on bacterial cellulose (BC), in which the electrostatic interaction of BC and ZIF8 nanofibers effectively resisted the aggregation of ZIF8 nanocrystals and suppressed the collapse of the porous carbon structure (Fig. 14a). Then, after carbonization, carbon nanofiber from BC and N-doped porous carbon nanoparticles from ZIF8 connected each other to construct a 3D network with silk cocoon-like node morphology, that is beneficial to expand electrochemical active sites and shorten ion diffusion length. Finally, the optimal carbonized aerogel NCNF2-900 fabricated an all-solid-state symmetric supercapacitor (SSC) which yielded a specific capacitance of 41.1 $F{\cdot}g^{-1}$ at 0.25 $A{\cdot}g^{-1}$ and retain a 5.7 $Wh{\cdot}Kg^{-1}$ energy density at a power density of 125 $W{\cdot}kg^{-1}$ (91% capacitance retention after 5000 cycles) (Fig. 14b, c). More interestingly, the carbonization of core-shell structured ZIF-8@ZIF-67 composites on a waste biomass cosmetic cotton was prepared by Xu and co-works to finally generate flexible N-doped carbon architectures (hetero-fNCs) with high supercapacitive properties, in which the pyrolysis of inter-layer ZIF-8 produced a large number of micropores [164], the outer-layer ZIF-67 brought rich mesopores and graphite microstructures, and cosmetic cotton derived carbon in the innermost layer offered more mechanical flexibility. Furthermore, hetero-fNCs showed a maximum density of 30 $Wh{\cdot}Kg^{-1}$ at a power density of 1440 $W{\cdot}kg^{-1}$ and good cycling stability (89.5% capacitance maintenance after 5000 cycles), indicating that N-doping in the carbon composites could enhance the capacitance owing to their ability of pseudo-capacitance contribution.

Apart from N-doping carbon architectures, metal sulfides and selenides encapsulated on hierarchical porous structure derived from ZIF-67 in biomass carbon have been done by Xiao's and Liu's groups [165, 166]. To explore the developed hierarchical porous metal derivatives from ZIFs as supercapacitors, Xiao et al. reported novel Ni_3S_2@-Co_9S_8/N-HPC composites [165], in which the strawberry-like Ni_3S_2@Co_9S_8 nanoparticles were obtained from in situ sulfuration progress of nickel alginate beads and ZIF-67 with a uniform distribution and were sealed in the 3D N-doping interconnected porous framework beneficial to high theoretical specific capacitance. And then high specific surface area and porous carbon structure from the biomass derived carbon enlarged the ion transport to improve conductivity of electrode materials. The resulting sample demonstrated a high specific capacitance of 1970.5 $F{\cdot}g^{-1}$ at 0.5 $A{\cdot}g^{-1}$ with asymmetric supercapacitor (ASC) exhibiting a maximum energy density of 77.1 $Wh{\cdot}kg^{-1}$ at 263.3 $W{\cdot}kg^{-1}$. Afterwards, ZIF/biomass-derived CoSe/C@C hierarchical composites were firstly fabricated by Liu et al. using ZIF-67 and CMC aerogel through the process of freeze-drying and selenization [167]. In this sample, lots of conductive pathways were provided by CoSe and C nanoparticles to drive fast ion passage. Additionally, the porous carbon network was in favor of relieving the volume pressure in charging and discharging. From the above results, it can be seen that the derived metal sulfides and selenides encapsulated on hierarchical structure from ZIFs and biomass carbon are promising electrode materials for SCs.

Conducting polymers have been considered as potential pseudocapacitive materials due to high capacitance, good conductivity and easy synthesis [168]. Among them, PANI has attracted more attentions because of wire conductive structure. However, the volume expansion and contraction of PANI can lead to fast capacitance decay. So PANI is often compounded with stable materials or fabricated particular structure. Guo's group reported a novel hybrid nanomaterial WS@Ni-MOF/SPANI, which was connected by Ni-MOF, carbonized walnut shells (WS) and vulcanized polyaniline (SPANI) [169]. 2D Ni-MOF and SPANI was in situ wrapped in the outer and inner channels of biomass

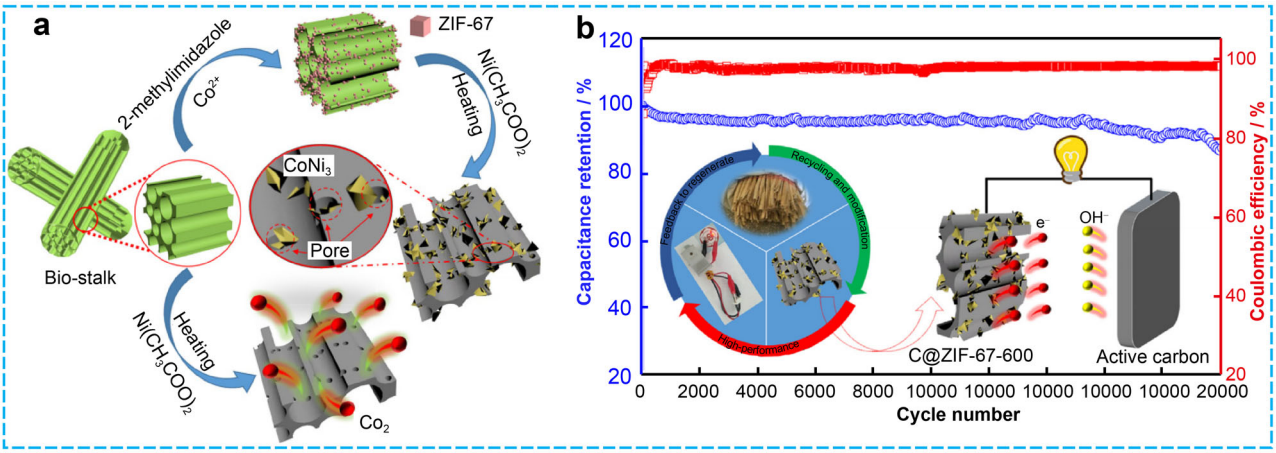

Fig. 13 Composite of honeycomb-like C@ZIF-67: **a** synthesis route of C@ZIF-67; **b** cycling performance and Coulombic efficiency of C@ZIF-67//AC device. Reproduced with permission from Ref. [162]. Copyright 2018, Elsevier Ltd.

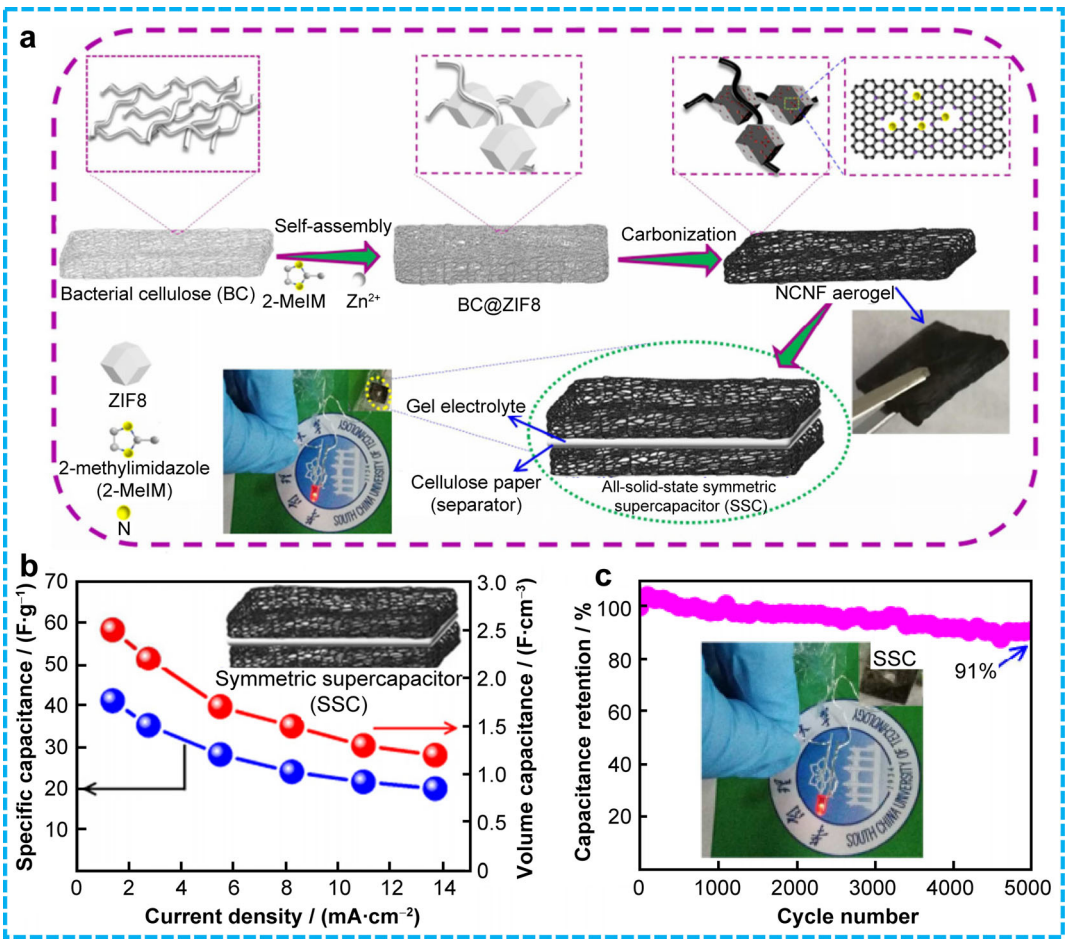

Fig. 14 BC@ZIF8 composite: **a** fabrication of all-sold-state symmetric supercapacitor based on BC and ZIF8; **b** SSC electrochemical performances and **c** cycle capability. Reproduced with permission from Ref. [163]. Copyright 2019, Elsevier Ltd.

derived carbon to accelerate ion transfer, in which SPANI played the role of a template to prevent the aggregation of MOF material to expose more active sites. The results indicate that the specific capacitance is up to 14 times that of biochar and maintains 90.4% capacitance retention after 20000 cycles. In addition, the ASC of WS@Ni-MOF/

SPANI//AC remained 34.79 $Wh{\cdot}kg^{-1}$ energy density at the power density of 824 $W{\cdot}kg^{-1}$.

To date, the synthesis method of biomass-derived carbon/MOFs composites mainly adopts in situ growth technology. For example, Huang et al. reported a family of MOFs@wood-derived hierarchical porous composites [170], the biomass wood slices were firstly treated by NaOH for the growth of MOFs, and the wood slices were soaked in the raw solution for synthesizing MOF. Then, the MOF particles in situ grew on the wood slices through interactions of hydrogen bonds and electrostatic. Finally, through carbonization, the 3D conductive carbon frameworks were fabricated by the wood precursor and MOFs were converted to heteroatoms-doped carbon with hollow polyhedrons. Through in situ growth method, the strong hydrogen bonds and electrostatic interactions between MOF and modified biomass materials inhibit the aggregation and microstructural collapse of MOFs during the pyrolysis [170]. Furthermore, there are also many techniques applied to the preparation of composite materials, such as hydro-thermal, directing mixing and so on. However, the reaction mechanisms of different preparation methods are rarely reported, and it will take a long time to realize the precise control of biomass-derived carbon/MOFs composites.

8 Conclusion and perspectives

Searching for suitable and excellent electrode materials of SCs is a worthwhile issue for electrical energy storage systems. Carbon materials, especially porous carbon, are considered as the commercially valued electrode material due to their high surface areas, adjusting porosity, good conductivity and stability. Additionally, biomass is a good precursor for preparing functional carbon materials as SCs electrode materials. Biomass precursors that can be used to make carbon material are agricultural crops and residues, forest materials, marine resources and wastes, industrial waste, and they provide an abundance of carbon composition and morphologies. The pore configuration of electrode materials is the most important factor to affect the power density and cycle life. The most desired hierarchical porous carbons contain at least two levels of pore sizes, in which mesopores and macropores provide copious channels for electron transfer. Up to now, many nanotechnologies provided facile and convenient way for the fabrication of high-quality biomass-derived carbon material, such as pyrolysis, hydrothermal carbonization, activation method. Though these nanotechnologies, the exquisite and complicated hierarchical nanostructures and morphologies have been obtained to provide more channels for conducting ions and electrons. In addition, as pseudocapacitive electrode materials, transition metal-based material can show higher power density and better stability because of variable valence and fast ion adsorption ability. Therefore, the combination of biomass-derived carbon and transition metal materials to fabricate electrodes can take full advantages of two materials to improve effective charge transfer, energy density and cycle life. In this review, we mainly focused on the recent progress and perspectives in the synthesis strategies and applications of biomass-derived carbon and their metal-based composites as electrode materials in supercapacitor application.

However, the development of biomass-derived carbonaceous material still faces many obstacles and challenges. Firstly, the primary components of biomass precursors need to be extracted from raw materials, but the existing separation technology can be limited by the toxicity, cost of chemicals and equipment. Secondly, the synthesis of the biomass derived porous carbon requires high-temperature carbonization technology at the most time; however, this approach is difficult to achieve tunable porosity and morphologies. Simultaneously, this low-efficiency energy utilization can bring serious environment problems. So far, some new strategies with no activation have been developed, such as soft- and hard templating, bio-template, mechanochemically-assisted method, but these approaches have not been widely used in practice. Finally, the structure, shape and morphologies of biomass carbon are difficult to be adjusted accurately, that may limit the rate performance and power density of electrode material. In addition, the effect of porosity of carbon materials on electrochemical properties is unclear.

Likewise, hybrid materials are designed by combining transition metal-based compounds (TMO, TMS, LDH, MOF) with biomass-derived carbon with synergy effect to give full play to the maximum advantages of each component in electrochemical performance. In general, although the porosity of composites decreases, the high capacitance can be obtained because of the increase of the metal content. In particular, polymetallic biomass-derived carbon composites manifest higher capacitance performance than bimetallic composites. Moreover, the problem of accumulation and aggregation between biomass-derived carbon skeleton and metal materials should be paid more attention in the process of preparation.

To sum up, although biomass-derived carbons/metal-based composites are a promising electrode material for energy storage devices, they still face great opportunities and challenges in the future. In order to promote the development of this field, future research should be focused on the following aspects:

Reasonable selection of biomass resource with high carbon content and low-cost is the crucial factor for sustainable utilization of biomass. Besides, accurate control of

the size, porosity, morphology and composition of biomass precursor can improve the performance of SCs.

In the preparation of biomass-derived carbons/metal-based composites, one significant challenge is how to explore simple, eco-environmentally and effective synthetic technology to avoid low-efficiency energy utilization and serious environment problems. In other words, future nanotechnology of composite electrode material for SCs cannot be limited in lab conditions, more practical and effective industrial synthesis methods should be seeked.

Most of the researches on biomass-derived carbons/metal-based composites as SCs focused on synthetic technology and practical application. The interaction mechanism and synergy effect on carbon matrix, metal and other doped-atoms are rarely reported. Therefore, further study of mechanism provides perspectives for deeper understanding of biomass-derived carbons/metal-based electrochemical materials.

Acknowledgments This study was financially supported by the National Natural Science of China (Nos. 22001156 and 21401121), General Financial Grant from the China Postdoctoral Science Foundation (No. 2017M623095), and Returned Personnel Science Foundation of Shaanxi Province, China (No. 2018044).

Declarations

Conflict of interests The authors declare that they have no conflict of interest.

References

[1] Simon P, Gogotsi Y. Materials for electrochemical capacitors. Nat Mater. 2008;7(11):845. https://doi.org/10.1038/nmat2297.
[2] Naskar P, Chakraborty P, Kundu D, Maiti A, Biswas B, Banerjee A. Envisaging future energy storage materials for supercapacitors: an ensemble of preliminary attempts. Chem Select. 2021;6(5):1127. https://doi.org/10.1002/slct.202100049.
[3] Gogotsi Y, Simon P. True performance metrics in electrochemical energy storage. Science. 2011;334(6058):917. https://doi.org/10.1126/science.1213003.
[4] Gu W, Yushin G. Review of nanostructured carbon materials for electrochemical capacitor applications: advantages and limitations of activated carbon, carbide-derived carbon, zeolite-templated carbon, carbon aerogels, carbon nanotubes, onion-like carbon, and graphene. Wiley Interdiscip Rev Energy Environ. 2014;3(5):424. https://doi.org/10.1002/wene.102.
[5] Thounthong P, Chunkag V, Sethakul P, Sikkabut S, Davat B. Energy management of fuel cell/solar cell/supercapacitor hybrid power source. J Power Sources. 2011;196(1):313. https://doi.org/10.1016/j.jpowsour.2010.01.051.
[6] Huang Y, Zhi CY. Functional flexible and wearable supercapacitors. J Phys D. 2017;50:273001. https://doi.org/10.1088/1361-6463/aa73b8.
[7] Wang YG, Song YF, Xia YY. Electrochemical capacitors: mechanism, materials systems, characterization and applications. Chem Soc Rev. 2016;45:5925. https://doi.org/10.1039/C5CS00580A.
[8] Bi Z, Kong Q, Cao Y, Sun G, Fangyuan S, Wei X, Li X, Ahmad A, Xie L, Chen CM. Biomass-derived porous carbon materials with different dimensions for supercapacitor electrodes: a review. J Mater Chem A. 2019;7(27):16028. https://doi.org/10.1039/C9TA04436A.
[9] Frackowiak E, Béguin F. Carbon materials for the electrochemical storage of energy in capacitors. Carbon. 2001;39(6):937. https://doi.org/10.1016/S0008-6223(00)00183-4.
[10] Lota G, Fic K, Frackowiak E. Carbon nanotubes and their composites in electrochemical applications. Energy Environ Sci. 2011;4:1592. https://doi.org/10.1039/C0EE00470G.
[11] Tao XY, Zhang XB, Zhang L, Cheng JP, Liu F, Luo JH, Luo ZQ, Geise HJ. Synthesis of multi-branched porous carbon nanofibers and their application in electrochemical double-layer capacitors-sciencedirect. Carbon. 2006;44(8):1425. https://doi.org/10.1016/j.carbon.2005.11.024.
[12] Xu C, Xu B, Gu Y, Xiong Z, Sun J, Zhao XS. Graphene-based electrodes for electrochemical energy storage. Energy Environ Sci. 2013;6:1388. https://doi.org/10.1039/C3EE23870A.
[13] Liu WJ, Ke T, Ling LL, Yu HQ, Hong J. Use of nutrient rich hydrophytes to create N, P-dually doped porous carbon with robust energy storage performance. Environ Sci Technol. 2016;50(22):12421. https://doi.org/10.1021/acs.est.6b03051.
[14] Paraknowitsch JP, Thomas A. Doping carbons beyond nitrogen: an overview of advanced heteroatom doped carbons with boron, sulphur and phosphorus for energy applications. Energy Environ Sci. 2013;6:2839. https://doi.org/10.1039/C3EE41444B.
[15] Huang WH, Chen Z, Wang HY, Wang L, Zhang HB, Wang H. Sponge-like hierarchical porous carbon decorated by Fe atoms for high-efficiency sodium storage and diffusion. Chem Commun. 2022;58(28):4496. https://doi.org/10.1039/D1CC07305B.
[16] Deng Y, Xie Y, Zou K, Ji X. Review on recent advances in nitrogen-doped carbons: preparations and applications in supercapacitors. J Mater Chem A. 2016;4:1144. https://doi.org/10.1039/C5TA08620E.
[17] Wang J, Nie P, Ding B, Dong SY, Hao XD, Dou H, Zhang XG. Biomass derived carbon for energy storage devices. J Mater Chem A. 2017;5:2411. https://doi.org/10.1039/C6TA08742F.
[18] Sun YQ, Wu QO, Shi GQ. Graphene based new energy materials. Energy Environ Sci. 2011;4:1113. https://doi.org/10.1039/C0EE00683A.
[19] Moon RJ, Martini A, Nairn J, Simonsen J, Youngblood J. Cellulose nanomaterials review: structure, properties and nanocomposites. Chem Soc Rev. 2011;40:3941. https://doi.org/10.1039/C0CS00108B.
[20] Ren YF, He ZL, Zhao HZ, Zhu T. Fabrication of MOF-derived mixed metal oxides with carbon residues for pseudocapacitors with long cycle life. Rare Metals. 2022;41(3):830. https://doi.org/10.1007/s12598-021-01836-8.
[21] Zhang Y, Liu S, Zheng X, Wang X, Xu Y, Tang H, Kang FY, Yang QH, Luo JY. Biomass carbonization: biomass organs control the porosity of their pyrolyzed carbon. Adv Funct Mater. 2017;27(3):1604687. https://doi.org/10.1002/adfm.201770025.
[22] Gao F, Jiangying Q, Geng C, Shao G, Mingbo W. Self-templating synthesis of nitrogen-decorated hierarchical porous carbon from shrimp shell for supercapacitors. J Mater Chem A. 2016;4(19):7445. https://doi.org/10.1039/C6TA01314G.
[23] Chen Z, Zhuo H, Hu Y, Zhong L, Peng X, Jing S, Sun R. Self-biotemplate preparation of hierarchical porous carbon with rational mesopore ratio and high oxygen content for an ultrahigh energy-density supercapacitor. ACS Sustain Chem Eng. 2018;6(5):7138.
[24] Song S, Ma F, Wu G, Ma D, Geng W, Wan J. Facile self-templating large scale preparation of biomass-derived 3d

hierarchical porous carbon for advanced supercapacitors. J Mater Chem. 2015;3:18154. https://doi.org/10.1039/C5TA04721H.
[25] Kim S, Park CB. Bio-inspired synthesis of minerals for energy, environment, and medicinal applications. Adv Funct Mater. 2013;23(1):10. https://doi.org/10.1002/adfm.201201994.
[26] Chen J, Fang K, Chen Q, Xu J, Wong C. Integrated paper electrodes derived from cotton stalks for high-performance flexible supercapacitors. Nano energy. 2018;53:337. https://doi.org/10.1016/j.nanoen.2018.08.056.
[27] Chen J, Chen M, Zhou W, Xinwu X, Liu B, Zhang W, Wong C. Simplified synthesis of fluoride-free $Ti_3C_2T_x$ via electrochemical etching toward high-performance electrochemical capacitors. ACS Nano. 2022;16(2):2461. https://doi.org/10.1021/acsnano.1c09004.
[28] Wang T, Kou Z, Zhang J, Wang H, Zeng YJ, Wei S, Zhang H. Boosting Faradic efficiency of dinitrogen reduction on the negatively charged Mo sites modulated via interstitial Fe doping into a Mo_2C nanowall catalyst. Chem Eng J. 2021;412:12861. https://doi.org/10.1016/j.cej.2020.127924.
[29] Quispe-Garrido V, Cerron-Calle GA, Bazan-Aguilar A, Ruiz-Montoya JG, Baena-Moncada AM. Advances in the design and application of transition metal oxide-based supercapacitors. Open Chemistry. 2021;19(1):709. https://doi.org/10.1515/chem-2021-0059.
[30] Huang Y, Zhu M, Huang Y, Li H, Pei Z, Xue Q, Zhi C. A modularization approach for linear-shaped functional supercapacitors. J Mater Chem. 2016;4:4580. https://doi.org/10.1039/C6TA00753H.
[31] Chen X, Wang H, Yi H, Wang X, Yan X, Guo Z. Anthraquinone on porous carbon nanotubes with improved supercapacitor performance. J Phys Chem C. 2014;118(16):8262. https://doi.org/10.1021/jp5009626.
[32] Wu ZS, Wang DW, Ren W, Zhao J, Zhou G, Li F, Cheng HM. Anchoring hydrous RuO_2 on graphene sheets for high-performance electrochemical capacitors. Adv Funct Mater. 2010;20(20):3595. https://doi.org/10.1002/adfm.201001054.
[33] Hu CC, Tsou TW. Ideal capacitive behavior of hydrous manganese oxide prepared by anodic deposition. Electrochem Commun. 2002;4(2):105. https://doi.org/10.1016/S1388-2481(01)00285-5.
[34] Xu J, He F, Gai S, Zhang S, Li L, Yang P. Nitrogen-enriched, double-shelled carbon/layered double hydroxide hollow microspheres for excellent electrochemical performance. Nanoscale. 2014;6:10887. https://doi.org/10.1039/C4NR02756F.
[35] Huang WH, Li XM, Yang XF, Zhang XX, Wang HH, Wang H. The recent progress and perspectives on metal- and covalent-organic framework based solid-state electrolytes for lithium-ion batteries. Mater Chem Front. 2021;5:3593. https://doi.org/10.1039/d0qm00936a.
[36] Li J, Yang M, Wei J, Zhou Z. Preparation and electrochemical performances of doughnut-like $Ni(OH)_2$.$Co(OH)_2$ composites as pseudocapacitor materials. Nanoscale. 2012;4:4498. https://doi.org/10.1039/C2NR30936J.
[37] Li J, Chen S, Zhu X, She X, Liu T, Zhang H, Yao X. Toward aerogel electrodes of superior rate performance in supercapacitors through engineered hollow nanoparticles of $NiCo_2O_4$. Adv Sci. 2017;4(12):1700345. https://doi.org/10.1002/advs.201700345.
[38] Zhang YN, Li L, Chen JL, Ma YM, Yang XW. MOFs template derived Co/Fe binary phosphide nanocomposite embedded in ternary-doped carbon matrix for efficient water splitting. Ceram Int. 2021;47(21):29535. https://doi.org/10.1016/j.ceramint.2021.01.145.
[39] Guo H, Feng Q, Kaiwen X, Jingsan X, Zhu J, Zhang C, Liu T. Self-templated conversion of metallogel into heterostructured TMP@carbon quasiaerogels boosting bifunctional electrocatalysis. Adv Funct Mater. 2019;29(34):1903660. https://doi.org/10.1002/adfm.201903660.
[40] Guo H, Zhou J, Li Q, Li Y, Zong W, Zhu J, Xu J, Zhang C, Liu T. Emerging dual-channel transition-metal-oxide quasiaerogels by self-embedded templating. Adv Funct Mater. 2020;30(15):2000024. https://doi.org/10.1002/adfm.202000024.
[41] Zhu T, Liu S, Wan K, Zhang C, Feng Y, Feng W, Liu T. Fluorine and nitrogen dual-doped porous carbon nanosheet-enabled compact electrode structure for high volumetric energy storage. ACS Appl Energy Mater. 2020;3:4949. https://doi.org/10.1021/acsaem.0c00500.
[42] Ruiz-Montoya JG, Quispe-Garrido VL, Gómez JC, Moncada AMB, Gonçalves JM. Recent progress in and prospects for supercapacitor materials based on metal oxide or hydroxide/biomass-derived carbon composites. Sustain Energy Fuels. 2021;5:5332. https://doi.org/10.1039/D1SE01170G.
[43] Biswal M, Banerjee A, Deo M, Ogale S. From dead leaves to high energy density supercapacitors. Energy Environ Sci. 2013;6(4):1249. https://doi.org/10.1039/C3EE22325F.
[44] Zhang Y, Liu X, Wang S, Li L, Dou S. Bio-nanotechnology in high-performance supercapacitors. Adv Energy Mater. 2017;7(21):1700592. https://doi.org/10.1002/aenm.201700592.
[45] Hao P, Zhao Z, Tian J, Li H, Sang Y, Guangwei Y, Cai H, Hong Liu C, Wong AU. Hierarchical porous carbon aerogel derived from bagasse for high performance supercapacitor electrode. Nanoscale. 2014;6(20):12120. https://doi.org/10.1039/C4NR03574G.
[46] Lu H, Zhao XS. Biomass-derived carbon electrode materials for supercapacitors. Sustain Energy Fuels. 2017;1:1265. https://doi.org/10.1039/C7SE00099E.
[47] Szczęśniaka B, Phuriragpitikhonb J, Chomaa J, Jaroniec M. Recent advances in the development and applications of biomass derived carbons with uniform porosity. J Mater Chem A. 2020;8:18464. https://doi.org/10.1039/D0TA05094F.
[48] Zhao X, Chen H, Kong F, Zhang Y, Wang S, Liu S, Lucia LA, Fatehi P, Pang H. Fabrication, characteristics and applications of carbon materials with different morphologies and porous structures produced from wood liquefaction: a review. Chem Eng J. 2019;364:226. https://doi.org/10.1016/j.cej.2019.01.159.
[49] Benaddi H, Legras D, Rouzaud JN, Beguin F. Influence of the atmosphere in the chemical activation of wood by phosphoric acid. Carbon. 1998;36:306. https://doi.org/10.1016/S0008-6223(98)80123-1.
[50] Foley NJ, Thomas KM, Forshaw PL, Stanton D, Norman PR. Kinetics of water vapor adsorption on activated carbon. Langmuir. 1997;13:2083. https://doi.org/10.1021/la960339s.
[51] Macías-García A, Díaz-Díez MA, Cuerda-Correa EM, Olivares-Marín M, Gañan-Gómez J. Study of the pore size distribution and fractal dimension of HNO_3-treated activated carbons. Appl Surf Sci. 2006;252(17):5972. https://doi.org/10.1016/j.apsusc.2005.11.010.
[52] Jin Y, Tian K, Wei L, Zhang X, Guo X. Hierarchically porous microspheres of activated carbon with high surface area from spores for electrochemical double-layer capacitors. J Mater Chem A. 2016;4:15968. https://doi.org/10.1039/C6TA05872H.
[53] Bin XU, Feng WU, Cao GP, Yang YS. Effect of carbonization temperature on microstructure of PAN-based activated carbon fibers prepared by CO_2 activation. New Carbon Mater. 2006;21(1):14. https://doi.org/10.1016/S1872-1508(06)60066-1.
[54] Xiong L, Wang XF, Li L, Jin L, Zhang YG, Song SL, Liu RP. Nitrogen-enriched porous carbon fiber as a CO_2 adsorbent with superior CO_2 selectivity by air activation. Energy & Fuels.

2019;33:12558. https://doi.org/10.1021/acs.energyfuels.9b02769.
[55] Li Z, Gu D, Liu Y, Wang H, Wang L. Recent advances and challenges in biomass-derived porous carbon nanomaterials for supercapacitors. Chem Eng J. 2020;397:125418. https://doi.org/10.1016/j.cej.2020.125418.
[56] Wang J, Kaskel S. KOH activation of carbon-based materials for energy storage. J Mater Chem. 2012;22:23710. https://doi.org/10.1039/C2JM34066F.
[57] Li Y, Zhang X, Yang R, Li G, Hu C. The role of H_3PO_4 in the preparation of activated carbon from NaOH-treated rice husk residue. RSC Advances. 2015;5:32626. https://doi.org/10.1039/C5RA04634C.
[58] Shi J, Cui H, Xu J, Yan N, Liu Y. Design and fabrication of hierarchically porous carbon frameworks with Fe_2O_3 cubes as hard template for CO_2 adsorption. Chem Eng J. 2020;389:124459. https://doi.org/10.1016/j.cej.2020.124459.
[59] Liu S, Zhao Y, Zhang B, Xia H, Zhou J, Xie W, Li H. Nano-micro carbon spheres anchored on porous carbon derived from dual-biomass as high rate performance supercapacitor electrodes. J Power Sources. 2018;381:116. https://doi.org/10.1016/j.jpowsour.2018.02.014.
[60] Liu R, Zhou A, Zhang X, Mu J, Che H, Wang Y, Wang T, Zhang Z, Kou Z. Fundamentals, advances and challenges of transition metal compounds-based supercapacitors. Chem Eng J. 2021;412:128611. https://doi.org/10.1016/j.cej.2021.128611.
[61] Pramitha A, Raviprakash Y. Recent developments and viable approaches for high-performance supercapacitors using transition metal-based electrode materials. J Energy Storage. 2022;49:104120. https://doi.org/10.1016/j.est.2022.104120.
[62] Wang R, Li X, Nie Z, Zhao Y, Wang H. Metal/metal oxide nanoparticles-composited porous carbon for high-performance supercapacitors. J Energy Storage. 2021;38: 102479. https://doi.org/10.1016/j.est.2021.102479.
[63] Gui Z, Zhu H, Gillette E, Han X, Rubloff GW, Hu L, Lee SB. Natural cellulose fiber as substrate for supercapacitor. ACS Nano. 2013;7(7):6037. https://doi.org/10.1021/nn401818t.
[64] Chen F, Zhou W, Yao H, Fan P, Yang J, Fei Z, Zhong M. Self-assembly of NiO nanoparticles in lignin-derived mesoporous carbons for supercapacitor applications. Green Chem. 2013;15:3057. https://doi.org/10.1039/C3GC41080C.
[65] Li Y, Zhao X, Xu Q, Zhang Q, Chen D. Facile preparation and enhanced capacitance of the polyaniline/sodium alginate nanofiber network for supercapacitors. Langmuir. 2011;27:6458. https://doi.org/10.1021/la2003063.
[66] Pushparaj VL, Shaijumon MM, Kumar A, Murugesan S, Ci L, Vajtai R, Ajayan PM. Flexible energy storage devices based on nanocomposite paper. Proc Natl Acad Sci USA. 2007;104:13574. https://doi.org/10.1073/pnas.0706508104.
[67] Mahadeva SK, Walus K, Stoeber B. Paper as a platform for sensing applications and other devices: a review. ACS Appl Mater Interfaces. 2015;7(16):8345. https://doi.org/10.1021/acsami.5b00373.
[68] Chee WK, Lim HN, Zainal Z, Huang NM, Harrison I, Andou Y. Flexible graphene-based supercapacitors: a review. Phys Chem C. 2016;120(8):4153. https://doi.org/10.1021/acs.jpcc.5b10187.
[69] He S, Chen W. 3D graphene nanomaterials for binder-free supercapacitors: scientific design for enhanced performance. Nanoscale. 2015;7:6957. https://doi.org/10.1039/C4NR05895J.
[70] Azadfalah M, Sedghi A, Hosseini H, Mirhosseini S. Synergic effect of physically-mixed metal organic framework based electrodes as a high efficient material for supercapacitors. J Energy Storage. 2021;44:103248. https://doi.org/10.1016/j.est.2021.103248.
[71] Ray A, Roy A, Saha S, Das S. Transition metal oxide-based nano-materials for energy storage application. Sci Technol Adv Appl Supercapacitors. 2019;1:17. https://doi.org/10.5772/intechopen.80298.
[72] Low WH, Khiew PS, Lim SS, Siong CW, Ezeigwe ER. Recent development of mixed transition metal oxide and graphene/mixed transition metal oxide based hybrid nanostructures for advanced supercapacitors. J Alloys Compd. 2019;775:1324. https://doi.org/10.1016/j.jallcom.2018.10.102.
[73] Zhang Y, Li L, Su H, Huang W, Dong X. Binary metal oxide: advanced energy storage materials in supercapacitors. J Mater Chem A. 2015;3:43. https://doi.org/10.1039/C4TA04996A.
[74] Veerakumar P, Sangili A, Manavalan S, Thanasekaran P, Lin KC. Research progress on porous carbon supported metal/metal oxide nanomaterials for supercapacitor electrode applications. Ind Eng Chem Res. 2020;59(14):6347. https://doi.org/10.1021/acs.iecr.9b06010.
[75] Liu N, Su Y, Wang Z, Wang Z, Xia J, Chen Y, Geng F. Electrostatic-interaction-assisted construction of 3D networks of manganese dioxide nanosheets for flexible high-performance solid-state asymmetric supercapacitors. ACS Nano. 2017;11(8):7879. https://doi.org/10.1021/acsnano.7b02344.
[76] Yang M, Kim DS, Hong SB, Sim JW, Kim J, Kim SS, Choi BG. MnO_2 nanowire/biomass-derived carbon from hemp stem for high-performance supercapacitors. Langmuir. 2017;33:5140. https://doi.org/10.1021/acs.langmuir.7b00589.
[77] Yu J, Li M, Wang X, Yang Z. Promising high-performance supercapacitor electrode materials from MnO_2 nanosheets@bamboo leaf carbon. ACS Omega. 2020;5(26):16299. https://doi.org/10.1021/acsomega.0c02169.
[78] Chen Q, Chen J, Zhou Y, Song C, Tian Q, Xu J, Wong CP. Enhancing pseudocapacitive kinetics of nanostructured MnO_2 through anchoring onto biomass-derived porous carbon. Appl Surf Sci. 2018;440:1027. https://doi.org/10.1016/j.apsusc.2018.01.224.
[79] Wang X, Chen S, Li D, Sun S, Peng Z, Komarneni S, Yang D. Direct interfacial growth of MnO_2 nanostructure on hierarchically porous carbon for high-performance asymmetric supercapacitors. ACS Sustain Chem Eng. 2018;6(1):633. https://doi.org/10.1021/acssuschemeng.7b02960.
[80] Hu X, Xiong W, Wang W, Qin S, Cheng H, Zeng Y, Zhu Z. Hierarchical manganese dioxide/poly(3,4-ethylenedioxythiophene) core–shell nanoflakes on ramie-derived carbon fiber for high-performance flexible all-solid-state supercapacitor. ACS Sustain Chem Eng. 2016;4(3):1201. https://doi.org/10.1021/acssuschemeng.5b01263.
[81] Zhao N, Deng L, Luo D, Zhang P. One-step fabrication of biomass-derived hierarchically porous carbon/MnO nanosheets composites for symmetric hybrid supercapacitor. Appl Surf Sci. 2020;526:146696. https://doi.org/10.1016/j.apsusc.2020.146696.
[82] Zhang H, Zhang Z, Qi X, Yu J, Cai J, Yang Z. Manganese monoxide/biomass-inherited porous carbon nanostructure composite based on the high water-absorbent agaric for asymmetric supercapacitor. ACS Sustain Chem Eng. 2019;7(4):4284. https://doi.org/10.1021/acssuschemeng.8b06049.
[83] Raj S, Srivastava SK, Kar P, Roy P. In situ growth of Co_3O_4 nanoflakes on reduced graphene oxide-wrapped Ni-foam as high performance asymmetric supercapacitor. Electrochimica Acta. 2019;302:327. https://doi.org/10.1016/j.electacta.2019.02.010.
[84] Li ZY, Bui PT, Kwak DH, Akhtar MS, Yang OB. Enhanced electrochemical activity of low temperature solution process synthesized Co_3O_4 nanoparticles for pseudo-supercapacitors applications. Ceram Int. 2016;42(1):1879. https://doi.org/10.1016/j.ceramint.2015.09.155.

[85] Zhou X, Shen X, Xia Z, Zhang Z, Li J, Ma Y, Qu Y. Hollow fluffy Co_3O_4 cages as efficient electroactive materials for supercapacitors and oxygen evolution reaction. ACS Appl Mater Interfaces. 2015;7(36):20322. https://doi.org/10.1021/acsami.5b05989.
[86] Zou R, Zhu L, Yan L, Shao B, Cheng H, Sun W. Co_3O_4 anchored on meshy biomass carbon derived from kelp for high-performance ultracapacitor electrode. Mater Chem Phys. 2021;266:124556. https://doi.org/10.1016/j.matchemphys.2021.124556.
[87] Zhao Y, Liu Y, Du J, Zhang X, Zhou J, Li X, Pan X. Facile synthesis of interconnected carbon network decorated with Co_3O_4 nanoparticles for potential supercapacitor applications. Appl Surf Sci. 2019;487:442. https://doi.org/10.1016/j.apsusc.2019.05.142.
[88] Xie X, Hou C, Wu D, Sun X, Yang X, Zhang Y, Du W. Facile synthesis of various Co_3O_4/bio-activated carbon electrodes for hybrid capacitor device application. J Alloys Compd. 2022;891:161967. https://doi.org/10.1016/j.jallcom.2021.161967.
[89] Ji Y, Deng Y, Chen F, Wang Z, Lin Y, Guan Z. Ultrathin Co_3O_4 nanosheets anchored on multi-heteroatom doped porous carbon derived from biowaste for high performance solid-state supercapacitors. Carbon. 2020;156:359. https://doi.org/10.1016/j.carbon.2019.09.064.
[90] Ning W, Chen L, Wei W, Chen Y, Zhang X. $NiCoO_2$/NiCoP@Ni nanowire arrays: tunable composition and unique structure design for high-performance winding asymmetric hybrid supercapacitors. Rare Metals. 2020;39:1034. https://doi.org/10.1007/s12598-020-01374-9.
[91] Wang G, Zhang L, Zhang J. A review of electrode materials for electrochemical supercapacitors. Chem Soc Rev. 2012;41:797. https://doi.org/10.1039/C1CS15060J.
[92] Zhao DD, Bao SJ, Zhou WJ, Li HL. Preparation of hexagonal nanoporous nickel hydroxide film and its application for electrochemical capacitor. Electrochem Commun. 2007;9(5):869. https://doi.org/10.1016/j.elecom.2006.11.030.
[93] Zhang S, Pang Y, Wang Y, Dong B, Lu S, Li M, Ding S. NiO nanosheets anchored on honeycomb porous carbon derived from wheat husk for symmetric supercapacitor with high performance. J Alloys Compd. 2018;735:1722. https://doi.org/10.1016/j.jallcom.2017.11.294.
[94] Paravannoor A. One-pot synthesis of biochar wrapped Ni/NiO nanobrick composites for supercapacitor applications. J Electroanal Chem. 2018;823:656. https://doi.org/10.1016/j.jelechem.2018.04.060.
[95] Lai F, Miao YE, Zuo L, Lu H, Huang Y, Liu T. Biomass-derived nitrogen-doped carbon nanofiber network: a facile template for decoration of ultrathin nickel-cobalt layered double hydroxide nanosheets as high-performance asymmetric supercapacitor electrode. Small. 2016;12(24):3235. https://doi.org/10.1002/smll.201600412.
[96] Kim DK, Hwang M, Ko D, Kang J, Seong KD, Piao Y. Electrochemical performance of 3D porous Ni-Co oxide with electrochemically exfoliated graphene for asymmetric supercapacitor applications. Electrochim Acta. 2017;246:680. https://doi.org/10.1016/j.electacta.2017.06.099.
[97] Veeramani V, Madhu R, Chen SM, Sivakumar M. Flower-like nickel–cobalt oxide decorated dopamine-derived carbon nanocomposite for high performance supercapacitor applications. ACS Sustain Chem Eng. 2016;4(9):5013. https://doi.org/10.1021/acssuschemeng.6b01391.
[98] Zhang C, Xie Z, Yang W, Liang Y, Meng D, He X, Zhang Z. $NiCo_2O_4$/biomass-derived carbon composites as anode for high-performance lithium ion batteries. J Power Sources. 2020;451:227761. https://doi.org/10.1016/j.jpowsour.2020.227761.
[99] Yang G, Park SJ. Nanoflower-like $NiCo_2O_4$ grown on biomass carbon coated nickel foam for asymmetric supercapacitor. J Alloys Compd. 2020;835:155270. https://doi.org/10.1016/j.jallcom.2020.155270.
[100] Nan J, Shi Y, Xiang Z, Wang S, Yang J, Zhang B. Ultrathin $NiCo_2O_4$ nanosheets assembled on biomass-derived carbon microsheets with polydopamine for high-performance hybrid supercapacitors. Electrochim Acta. 2019;301:107. https://doi.org/10.1016/j.electacta.2019.01.167.
[101] Nithya VD, Arul NS. Progress and development of Fe_3O_4 electrodes for supercapacitors. J Mater Chem A. 2016;4:10767. https://doi.org/10.1039/C6TA02582J.
[102] Lu XF, Chen XY, Zhou W, Tong YX, Li GR. α-Fe_2O_3@ PANI core–shell nanowire arrays as negative electrodes for asymmetric supercapacitors. ACS Appl Mater Interf. 2015;7(27):14843. https://doi.org/10.1021/acsami.5b03126.
[103] Pardieu E, Pronkin S, Dolci M, Dintzer T, Pichon BP, Begin D, Boulmedais F. Hybrid layer-by-layer composites based on a conducting polyelectrolyte and Fe_3O_4 nanostructures grafted onto graphene for supercapacitor application. J Mater Chem A. 2015;3:22877. https://doi.org/10.1039/C5TA05132K.
[104] Yu SH, Conte DE, Baek S, Lee DC, Park SK, Lee KJ, Pinna N. Structure-properties relationship in iron oxide-reduced graphene oxide nanostructures for Li-ion batteries. Adv Funct Mater. 2013;23(35):4293. https://doi.org/10.1002/adfm.201300190.
[105] Fang K, Chen J, Zhou X, Mei C, Tian Q, Xu J, Wong CP. Decorating biomass-derived porous carbon with Fe_2O_3 ultrathin film for high-performance supercapacitors. Electrochim Acta. 2018;261:198. https://doi.org/10.1016/j.electacta.2017.12.140.
[106] Wu XL, Wen T, Guo HL, Yang S, Wang X, Xu AW. Biomass-derived sponge-like carbonaceous hydrogels and aerogels for supercapacitors. ACS Nano. 2013;7(4):3589. https://doi.org/10.1021/nn400566d.
[107] Makkar P, Malik A, Ghosh NN. Biomass-derived porous carbon-anchoring $MnFe_2O_4$ hollow sphere and needle-like NiS for a flexible all-solid-state asymmetric supercapacitor. ACS Appl Energy Mater. 2021;4(6):6015. https://doi.org/10.1021/acsaem.1c00871.
[108] Gao Y, Zhao L. Review on recent advances in nanostructured transition-metal-sulfide-based electrode materials for cathode materials of asymmetric supercapacitors. Chem Eng J. 2022;430:132745. https://doi.org/10.1016/j.cej.2021.132745.
[109] Lu ZW, Zhang Y, Sun M, Zou P, Wang X, Wang Y, Huang Q, Chen H, Ye J, Rao H. N-doped carbon dots regulate porous hollow nickel-cobalt sulfide: high-performance electrode materials in supercapacitor and enzymeless glucose sensor. J Power Sources. 2021;516:230685. https://doi.org/10.1016/j.jpowsour.2021.230685.
[110] Hekmat F, Hosseini H, Shahrokhian S, Unalan HE. Hybrid energy storage device from binder-free zinc-cobalt sulfide decorated biomass-derived carbon microspheres and pyrolyzed polyaniline nanotube-iron oxide. Energy Stor Mater. 2020;25:621. https://doi.org/10.1016/j.ensm.2019.09.022.
[111] Fan G, Li F, Evans DG, Duan X. Catalytic applications of layered double hydroxides: recent advances and perspectives. Chem Soc Rev. 2014;43:7040. https://doi.org/10.1039/C4CS00160E.
[112] Qin K, Wang L, Wen S, Diao L, Liu P, Li J, Zhao N. Designed synthesis of NiCo-LDH and derived sulfide on heteroatom-doped edge-enriched 3D rivet graphene films for high-performance asymmetric supercapacitor and efficient OER. J Mater Chem A. 2018;6:8109. https://doi.org/10.1039/C8TA01832D.

[113] Jia H, Wang Z, Zheng X, Lin J, Liang H, Cai Y, Fei W. Interlaced Ni-Co LDH nanosheets wrapped Co_9S_8 nanotube with hierarchical structure toward high performance supercapacitors. Chem Eng J. 2018;351:348. https://doi.org/10.1016/j.cej.2018.06.113.
[114] Zhi L, Zhang W, Dang L, Sun J, Shi F, Xu H, Lei Z. Holey nickel cobalt layered double hydroxide thin sheets with ultra high areal capacitance. J Power Sources. 2018;387:108. https://doi.org/10.1016/j.jpowsour.2018.03.063.
[115] Huang B, Wang W, Pu T, Li J, Zhu J, Zhao C, Chen L. Two dimensional porous (Co, Ni)-based monometallic hydroxides and bimetallic layered double hydroxides thin sheets with honeycomb-like nanostructure as positive electrode for high-performance hybrid supercapacitors. J Colloid Interf Sci. 2018;532:630. https://doi.org/10.1016/j.jcis.2018.08.019.
[116] Li T, Li GH, Li LH, Liu L, Xu Y, Ding HY, Zhang T. Large-scale self assembly of 3D flower-like hierarchical Ni/Co-LDHs microspheres for high-performance flexible asymmetric supercapacitors. ACS Appl Mater Interf. 2016;8(4):2562. https://doi.org/10.1021/acsami.5b10158.
[117] Wu S, Hui KS, Hui KN, Kim KH. Electrostatic-induced assembly of graphene-encapsulated carbon@nickel aluminum layered double hydroxide core shell spheres hybrid structure for high-energy and high-power-density asymmetric supercapacitor. ACS Appl Mater Interf. 2017;9(2):1395. https://doi.org/10.1021/acsami.6b09355.
[118] Wimalasiri Y, Fan R, Zhao XS, Zou L. Assembly of Ni-Al layered double hydroxide and graphene electrodes for supercapacitors. Electrochim Acta. 2014;134:127. https://doi.org/10.1016/j.electacta.2014.04.129.
[119] Wang J, Song Y, Li Z, Liu Q, Zhou J, Jing X, Jiang Z. In situ Ni/Al layered double hydroxide and its electrochemical capacitance performance. Energy Fuel. 2010;24(12):6463. https://doi.org/10.1021/ef101150b.
[120] Zhao J, Chen J, Xu S, Shao M, Zhang Q, Wei F, Duan X. Hierarchical NiMn layered double hydroxide/carbon nanotubes architecture with superb energy density for flexible supercapacitors. Adv Funct Mater. 2014;24(20):2938. https://doi.org/10.1002/adfm.201303638.
[121] Gao J, Xuan H, Xu Y, Liang T, Han X, Yang J, Du Y. Interconnected network of zinc-cobalt layered double hydroxide stick onto rGO/nickel foam for high performance asymmetric supercapacitors. Electrochim Acta. 2018;286:92. https://doi.org/10.1016/j.electacta.2018.08.043.
[122] Yu J, Wang Q, O'Hare D, Sun L. Preparation of two dimensional layered double hydroxide nanosheets and their applications. Chem Soc Rev. 2017;46:5950. https://doi.org/10.1039/C7CS00318H.
[123] Li X, Du D, Zhang Y, Xing W, Xue Q, Yan Z. Layered double hydroxides toward high-performance supercapacitors. J Mater Chem A. 2017;5:15460. https://doi.org/10.1039/C7TA04001F.
[124] Cao Y, Li G, Li X. Graphene/layered double hydroxide nanocomposite: properties, synthesis, and applications. Chem Eng J. 2016;292:207. https://doi.org/10.1016/j.cej.2016.01.114.
[125] Wang HY, Shi GQ. Layered double hydroxide/graphene composites and their applications for energy storage and conversion. Acta Phys Chim Sin. 2018;34(1):22.
[126] Patel R, Park JT, Patel M, Dash JK, Bhoje Gowd E, Karpoormath R, Mishra A, Kwak J, Kim JH. Transition-metal-based layered double hydroxides tailored for energy conversion and storage. J Mater Chem A. 2018;6(1):12. https://doi.org/10.1039/C7TA09370E.
[127] Zhao M, Zhao Q, Li B, Xue H, Pang H, Chen C. Recent progress in layered double hydroxide based materials for electrochemical capacitors: design, synthesis and performance. Nanoscale. 2017;9:15206. https://doi.org/10.1039/C7NR04752E.
[128] Cheng JP, Zhang J, Liu F. Recent development of metal hydroxides as electrode material of electrochemical capacitors. RSC Adv. 2014;4:38893. https://doi.org/10.1039/C4RA06738J.
[129] Jiang L, Sheng L, Fan Z. Biomass-derived carbon materials with structural diversities and their applications in energy storage. Sci China Mater. 2018;61:133. https://doi.org/10.1007/s40843-017-9169-4.
[130] Golmohammadi F, Amiri M. Biomass-derived graphene-based nanocomposite: a facile template for decoration of ultrathin nickel–aluminum layered double hydroxide nanosheets as high-performance supercapacitors. Int J Hydrog Energy. 2020;45(31):15578. https://doi.org/10.1016/j.ijhydene.2020.04.044.
[131] Ma M, Cai W, Chen Y, Li Y, Tan F, Zhou J. Flower-like NiMn-layered double hydroxide microspheres coated on biomass-derived 3D honeycomb porous carbon for high-energy hybrid supercapacitors. Ind Crops Prod. 2021;166:113472. https://doi.org/10.1016/j.indcrop.2021.113472.
[132] Dong L, Xu C, Li Y, Huang ZH, Kang F, Yang QH, Zhao X. Flexible electrodes and supercapacitors for wearable energy storage: a review by category. J Mater Chem A. 2016;4:4659. https://doi.org/10.1039/C5TA10582J.
[133] Chen J, Wang X, Wang J, Lee PS. Sulfidation of NiMn-layered double hydroxides/graphene oxide composites toward supercapacitor electrodes with enhanced performance. Adv Energy Mater. 2016;6(5):1501745. https://doi.org/10.1002/aenm.201501745.
[134] Li S, Yu C, Yang J, Zhao C, Zhang M, Huang H, Qiu J. A superhydrophilic "nanoglue" for stabilizing metal hydroxides onto carbon materials for high-energy and ultralong-life asymmetric supercapacitors. Energy Environ Sci. 2017;10:1958. https://doi.org/10.1039/C7EE01040K.
[135] Lei W, Jin D, Liu H, Tong Z, Zhang H. An overview of bacterial cellulose in flexible electrochemical energy storage. ChemSusChem. 2020;13(15):3731. https://doi.org/10.1002/cssc.202001019.
[136] Wu ZY, Liang HW, Chen LF, Hu BC, Yu SH. Bacterial cellulose: a robust platform for design of three dimensional carbon-based functional nanomaterials. Acc Chem Res. 2016;49(1):96. https://doi.org/10.1021/acs.accounts.5b00380.
[137] Liu K, Liu Y, Lin D, Pei A, Cui Y. Materials for lithium-ion battery safety. Sci Adv. 2018. https://doi.org/10.1126/sciadv.aas9820.
[138] Zhu YS, Xiao SY, Li MX, Chang Z, Wang FX, Gao J, Wu YP. Natural macromolecule based carboxymethyl cellulose as a gel polymer electrolyte with adjustable porosity for lithium ion batteries. J Power Sources. 2015;288:368. https://doi.org/10.1016/j.jpowsour.2015.04.117.
[139] Zhao S, Zeng L, Cheng G, Yu L, Zeng H. Ni/Co-based metal-organic frameworks as electrode material for high performance supercapacitors. Chin Chem Lett. 2019;30(3):605. https://doi.org/10.1016/j.cclet.2018.10.018.
[140] Wu H, Zhang Y, Yuan W, Zhao Y, Luo S, Yuan X, Cheng L. Highly flexible, foldable and stretchable Ni-Co layered double hydroxide/polyaniline/bacterial cellulose electrodes for high-performance all-solid-state supercapacitors. J Mater Chem A. 2018;6:16617. https://doi.org/10.1039/C8TA05673K.
[141] Yuan Y, Zhou J, Rafiq MI, Dai S, Tang J, Tang W. Growth of NiMn layered double hydroxide and polypyrrole on bacterial cellulose nanofibers for efficient supercapacitors. Electrochim Acta. 2019;295:82. https://doi.org/10.1016/j.electacta.2018.10.090.
[142] Zhang Y, Zuo L, Zhang L, Yan J, Lu H, Fan W, Liu T. Immobilization of NiS nanoparticles on N-doped carbon fiber

aerogels as advanced electrode materials for supercapacitors. Nano Res. 2016;9:2747. https://doi.org/10.1007/s12274-016-1163-1.
[143] Shen L, Wang J, Xu G, Li H, Dou H, Zhang X. $NiCo_2S_4$ nanosheets grown on nitrogen-doped carbon foams as an advanced electrode for supercapacitors. Adv Energy Mater. 2015;5(3):1400977.
[144] Yan C, Chen G, Zhou X, Sun J, Lv C. Template-based engineering of carbon-doped Co_3O_4 hollow nanofibers as anode materials for lithium-ion batteries. Adv Funct Mater. 2016;26(9):1428. https://doi.org/10.1002/adfm.201504695.
[145] Zhou W, Cao X, Zeng Z, Shi W, Zhu Y, Yan Q, Zhang H. One-step synthesis of Ni_3S_2 nanorod@$Ni(OH)_2$ nanosheet core–shell nanostructures on a three-dimensional graphene network for high-performance supercapacitors. Energy Environ Sci. 2013;6:2216. https://doi.org/10.1039/C3EE40155C.
[146] Gao Y, Zhang L. Review on recent advances in nanostructured transition-metal-sulfide-based electrode materials for cathode materials of asymmetric supercapacitors. Chem Eng J. 2022;430:132745. https://doi.org/10.1016/j.cej.2021.132745.
[147] Lin S, Li H, Wu ZQ, Chen Q, Zhu L, Li CD, Zhu XB, Sun YP. Magneto-electrodeposition of 3D cross-linked NiCo-LDH for flexible high-performance supercapacitors. Small Methods. 2022;6(3):2101320. https://doi.org/10.1002/smtd.202101320.
[148] Zhang Y, Yu L, Hu R, Zhang J, Wang Y, Niu R, Zhu J. Biomass-derived C/N Co-doped $Ni(OH)_2/Ni_xS_y$ with a sandwich structure for supercapacitors. J Mater Chem A. 2018;6:17417. https://doi.org/10.1039/C8TA06072J.
[149] Xu L, Liang HW, Li HH, Wang K, Yang Y, Song LT, Yu SH. Understanding the stability and reactivity of ultrathin tellurium nanowires in solution: an emerging platform for chemical transformation and material design. Nano Res. 2015;8:1081. https://doi.org/10.1007/s12274-014-0586-9.
[150] Xu L, Liang HW, Yang Y, Yu SH. Stability and reactivity: positive and negative aspects for nanoparticle processing. Chem Rev. 2018;118(7):3209. https://doi.org/10.1021/acs.chemrev.7b00208.
[151] Ma X, Lou Y, Chen XB, Shi Z, Xu Y. Multifunctional flexible composite aerogels constructed through in-situ growth of metal-organic framework nanoparticles on bacterial cellulose. Chem Eng J. 2019;356:227. https://doi.org/10.1016/j.cej.2018.09.034.
[152] Tang Z, Zhang G, Zhang H, Wang L, Shi H, Wei D, Duan H. MOF-derived N-doped carbon bubbles on carbon tube arrays for flexible high-rate supercapacitors. Energy Storage Mater. 2018;10:75. https://doi.org/10.1016/j.ensm.2017.08.009.
[153] Liu C, Bai Y, Li W, Yang F, Zhang G, Pang H. In situ growth of three-dimensional MXene/metal–organic framework composites for high-performance supercapacitors. Angew Chem Int Ed. 2022;61(11):e202116282. https://doi.org/10.1002/anie.202116282.
[154] Bai Y, Liu C, Li W, Zheng S, Pi Y, Luo Y, Pang H. MXene-copper/cobalt hybrids via Lewis acidic molten salts etching for high performance symmetric supercapacitors. Angew Chem Int Ed. 2021;60(48):25318. https://doi.org/10.1002/anie.202116282.
[155] Zheng S, Li Q, Xue H, Pang H, Xu Q. A highly alkaline-stable metal oxide@metal–organic framework composite for high-performance electrochemical energy storage. Natl Sci Rev. 2020;7(2):305. https://doi.org/10.1093/nsr/nwz137.
[156] Li W, Guo X, Geng P, Meng D, Jing Q, Chen X, Zhang G, Li H, Qiang X, Braunstein P, Pang H. Rational design and general synthesis of multimetallic metal–organic framework nano-octahedra for enhanced Li–S battery. Adv Mater. 2021;33(45):2105163. https://doi.org/10.1002/adma.202105163.
[157] Munn AS, Dunne PW, Tang SVY, Lester EH. Large-scale continuous hydrothermal production and activation of ZIF-8. Chem Commun. 2015;5:12811. https://doi.org/10.1039/C5CC04636J.
[158] Wang L, Feng X, Ren L, Piao Q, Zhong J, Wang Y, Wang B. Flexible solid-state supercapacitor based on a metal–organic framework interwoven by electrochemically-deposited PANI. J Am Chem Soc. 2015;137(15):4920. https://doi.org/10.1021/jacs.5b01613.
[159] Yilmaz G, Yam KM, Zhang C, Fan HJ, Ho GW. In situ transformation of MOFs into layered double hydroxide embedded metal sulfides for improved electrocatalytic and supercapacitive performance. Adv Mater. 2017;29(26):1606814. https://doi.org/10.1002/adma.201606814.
[160] Wang Y, Liu T, Lin X, Chen H, Chen S, Jiang Z, Chen Y, Liu J, Huang J, Liu M. Self-templated synthesis of hierarchically porous n-doped carbon derived from biomass for supercapacitors. ACS Sustainable Chem Eng. 2018;6:13932. https://doi.org/10.1021/acssuschemeng.8b02255.
[161] Du W, Bai YL, Xu J, Zhao H, Zhang L, Li X, Zhang J. Advanced metal-organic frameworks (MOFs) and their derived electrode materials for supercapacitors. J Power Sources. 2018;402:281. https://doi.org/10.1016/j.jpowsour.2018.09.023.
[162] Yue L, Chen L, Liu X, Lu D, Zhou W, Li Y. Honeycomb-like biomass carbon with planted $CoNi_3$ alloys to form hierarchical composites for high-performance supercapacitors. J Colloid Interf Sci. 2022;608:2602. https://doi.org/10.1016/j.jcis.2021.10.184.
[163] Chen H, Liu T, Mou J, Zhang W, Jiang Z, Liu J, Liu M. Free-standing N-self-doped carbon nanofiber aerogels for high-performance all-solid-state supercapacitors. Nano Energy. 2019;63:103836. https://doi.org/10.1016/j.nanoen.2019.06.032.
[164] Zhao G, Xu X, Zhu G, Shi J, Li Y, Zhang S, Yamauchi Y. Flexible nitrogen-doped carbon heteroarchitecture derived from ZIF-8/ZIF-67 hybrid coating on cotton biomass waste with high supercapacitive properties. Microporous Mesoporous Mater. 2020;303: 110257. https://doi.org/10.1016/j.micromeso.2020.110257.
[165] Wang S, Xiao Z, Zhai S, Wang H, Cai W, Qin L, An Q. Construction of strawberry-like Ni_3S_2@Co_9S_8 heteronanoparticle-embedded biomass-derived 3D N-doped hierarchical porous carbon for ultrahigh energy density supercapacitors. J Mater Chem A. 2019;7:17345. https://doi.org/10.1039/C9TA05145G.
[166] Zhang X, He P, Dong B, Mu N, Liu Y, Yang T, Mi R. Synthesis and characterization of metal-organic framework/biomass-derived CoSe/C@C hierarchical structures with excellent sodium storage performance. Nanoscale. 2021;13:4167. https://doi.org/10.1039/D0NR08569C.
[167] Zhang X, He P, Dong B, Nan M, Liu Y, Yang T, Mi R. Synthesis and characterization of metal–organic framework/biomass-derived CoSe/C@C hierarchical structures with excellent sodium storage performance. Nanoscale. 2021;13(7):4167. https://doi.org/10.1039/D0NR08569C.
[168] Liu X, Zheng Y, Wang X. Controllable preparation of polyaniline–graphene nanocomposites using functionalized graphene for supercapacitor electrodes. Chem Eur J. 2015;21(29):10408. https://doi.org/10.1002/chem.201501245.
[169] Zhang J, Guo H, Yang F, Wang M, Zhang H, Zhang T, Yang W. Walnut shell-derived porous carbon integrated with Ni-MOF/SPANI composites for high-performance supercapacitor. Colloids Surfaces A: Physicochem Eng Asp. 2021;630: 127584. https://doi.org/10.1016/j.colsurfa.2021.127584.

[170] Zhang W, Li M, Zhong L, Huang J, Liu M. A family of MOFs@wood-derived hierarchical porous composites as free-standing thick electrodes of solid supercapacitors with enhanced areal capacitances and energy densities. Mater Today Energy. 2022;24:100951. https://doi.org/10.1016/j.mtener.2022.100951.